

Abstract

Human-wildlife conflict, characterized by road/railway accidents and crop damage, is a global challenge. This B-tech Project proposes an innovative solution: a battery-powered ultrasonic sound generator for animal deterrence. The system detects animal movement and emits high-frequency ultrasonic sound waves to repel animals from roads, railways, airports, or cultivated fields. The system is charged automatically by a PV panel, making it suitable for remote areas with limited access to electricity.

Currently, there is no commercially available wildlife pathway alert system that can detect, identify, and alert drivers/animals for the safety of both wildlife and humans. This project aims to reduce the chances of animal-vehicle collisions and save lives, especially for larger mammals like Bengal tigers, Indian elephants, and giraffes that are increasingly becoming casualties of road/railway accidents.

The proposed system offers several advantages, including its non-lethal and humane approach to animal deterrence, supporting wildlife conservation efforts and crop protection. It can also assist wildlife officers in managing wild animals and preventing animal-human conflicts in protected areas. Field testing can be conducted to evaluate its effectiveness in deterring animals and preventing wildlife-related incidents, providing real-world validation for the research.

In conclusion, the PV-powered ultrasonic sound generator offers an eco-friendly and humane solution to address human-wildlife conflict. This innovative system has the potential to contribute to wildlife conservation, crop protection, and wildlife management, providing practical solutions for real-life challenges.

Keywords: Ultrasonic sound generator, PV panel, battery, animal deterrence, wildlife conservation, crop protection, eco-friendly, human-wildlife conflict, animal casualties, wildlife management.

Contents

Certification of Approval	i
Certificate	ii
Declaration	iii
Acknowledgments	iv
Abstract	v
List of Figures	ix
List of Abbreviations	xiii
1 Introduction	1
1.1 Proposed System	2
1.2 Organisation of Thesis	3
2 System Architecture	6
2.1 Powering the system	7
2.2 Selection of ultrasonic speaker	7
2.3 Animal detection	9
3 System Simulation	10

3.1	Charging the battery	10
3.1.1	MPPT algorithm	10
3.1.2	Simulating MPPT Buck converter	12
3.2	Powering Load & speaker	13
3.2.1	Boost converter switch as amplifier	13
3.3	BMS & Load Shortcircuit Protection	15
4	Circuit Design	16
4.1	Description of Microcontroller	16
4.1.1	Arduino Nano	17
4.1.2	Technical Specifications of Arduino Nano	17
4.1.3	Input and Output Pins of Arduino Nano	17
4.1.4	Powering the Arduino Nano	19
4.2	Voltage and Current Measurement	20
4.2.1	Voltage measurement	20
4.2.2	Current measurement	21
4.3	Power Inductor and Capacitor Selection	22
4.3.1	Power Inductor Selection	22
4.3.2	Capacitor selection	22
4.4	Converters Design Considerations	23
4.4.1	Selection of Power Switches & Diodes	23
4.4.2	Need for MOSFET Gate driver	25

4.5	Converters Design	26
4.5.1	Boost Converter	26
4.5.2	Buck Converter	27
4.6	Project Schematic	36
4.7	PCB Designing	37
4.7.1	Specifications	38
4.8	Other Features of the board	39
5	Testing	40
5.1	MPPT Testing	40
5.2	Boost converter & ultrasonic speaker Testing	42
5.3	Testing On Animals	44
6	Code Overview & Functionality	46
Conclusion		48
Bibliography		50

List of Figures

2.1	Proposed system architecture Block diagram	6
2.2	approx equivalent circuit and commercial Piezoelectric speaker	7
2.3	speaker Experimental setup, voltage applied(azure) and current drawn by speaker(Blue)	8
2.4	observed spectrum at 10KHz	8
3.1	Voltage,Current and power curve for a PV	11
3.2	P/O algorithm for MPP Operation	11
3.3	Simulation of MPPT charge controller	12
3.4	Voltage, current, and power output Vs Time of PV @1000W/m ²	12
3.5	power Vs Voltage of PV @1000W/m ²	13
3.6	Boost converter with speaker connected ac cross switch	14
3.7	Speaker voltage,Currents & Load Voltage Vs Time	14
3.8	Battery Over-voltage,Over-current, Reverse voltage protection by a Fuse and High-power Zener diode	15
4.1	Layout of Arduino Nano Board Top view	17
4.2	Power Tree of Arduino Nano (image taken from arduino usermanual) . .	18
4.3	Schematic for mp2307	19

4.4	Schematic for voltage measurement using Resistive divider Technique	20
4.5	Simulation for Current Measurement	21
4.6	Capacitor types and ranges	22
4.7	Three Dimensions of Power Transistor Applications	24
4.8	Boost Converter Circuit Schematic	26
4.9	Boost Converter Circuit Test Setup	26
4.10	V_{DS} (Azure) & $I_{Speaker}$ (Blue) Vs Time	27
4.11	$V_{Speaker}$ (Pink) Vs Time	27
4.12	Schematic Diagram and Experimental Setup for Buck converter by Bootstrapping	28
4.13	Simulation Schematic Diagram for Bootstrapping Pre-charge Circuit	29
4.14	Schematic for Bootstrapping operation by using voltage regulator	30
4.15	Simulation Schematic Diagram for Transformer-coupled gate driver	31
4.16	Schematic Diagram for Gate driver driven by isolated Power Supply	32
4.17	Schematic Diagram for BJT based Buck converter and Designed Circuit	33
4.18	Gate driver circuit for P-MOSFET Buck converter High side Switching	34
4.19	Setup for Buck converter based MPPT charge controller and results	35
4.20	Gate driver circuit for Boost-converter N-MOSFET Low side Switching	35
4.21	Project Schematic	36
4.22	Snapshot of PCB layout while designing for the Project	37
4.23	Project PCB after fabrication and Components assembly	37
4.24	List of Materials used in the Project PCB	38

5.1	Experimental Setup for MPPT and Load Test	40
5.2	Results For MPPT Test	41
5.3	V_D (Azure) & V_G (Blue) with respective ground for PV Buck converter .	41
5.4	V_{GS} (Left) & V_{DS} (Right) for PV Buck converter	41
5.5	V_{out} characteristics @ 60Khz	42
5.6	V_{out} characteristics @ fs = 12-60Khz of 2 sec repeated Linear sweep . .	42
5.7	V_{DS} / $V_{Speaker}$ & $I_{Speaker}$ vs Time	43
5.8	Parameter Readings from Arduino Serial Monitor	43
5.9	Ultrasonic Test On animals representing animal deterrence to Ultrasonic Sound	45

List of Tables

1.1	Animal hearing spectrum ranges	3
4.1	Technical specifications of Arduino Nano	17
4.2	Specifications of the Project Prototype	38

List of Abbreviations

AVG	animal-vehicle collisions
PV	Photo voltaic
MPPT	Maximum power point tracking
(P&O)	Perturb and Observe
BMS	Battery Management system
CC-CV	constant current constant voltage
PIR	passive infrared sensor
SoC	State of Charge
PCB	Printed Circuit Board
OP-amp	Operational amplifier
SPI	serial peripheral interface
I2C	Inter-Integrated Circuit pronounced as eye-squared-C
ADC	Analog to digital converter
EMI	Electromagnetic interference

Chapter 1

Introduction

Millions of wild animals are killed due to wildlife-vehicle collisions (AVCs) worldwide, with most incidents occurring at night in poorly lit areas, particularly on rural roads with low traffic. The lack of systematic monitoring for animal road-kill events often results in underestimation of the prediction of AVC incidents and costs at regional and national scales. In India, where highways and roads pass through protected wildlife areas, wildlife entering the road or railway tracks often leads to fatal accidents for both animals and humans. In India, a total of 752 incidences of mortality belonging to 17 species were recorded, with road and railway accidents accounting for 17.287% of the incidents. Mortalities due to accidents were highest during 2015-2016, with 37 recorded cases, and lowest during 2019-2020, with 22 cases. Among the road kills, mammals accounted for 96.923% of the incidents, while reptiles made up 3.076%. Notably, wild elephants (*Elephas maximus*) were identified as the major victims of vehicular collisions, with 39 individuals losing their lives in such accidents. These findings highlight the significant impact of road and railway accidents on wildlife mortality in India and the need for effective measures to mitigate wildlife-vehicle collisions and reduce the loss of endangered species such as wild elephants.

Additionally, crop damage caused by animal attacks poses a significant threat to crop yield. As human cultivation expands into previously wild areas, conflicts between

humans and wildlife, such as crop raiding, intensify. This paper aims to present our project on an ultrasonic sound generator, and its potential applications in deterring animals to reduce wildlife casualties due to road/railway accidents and protect crops from animal damage, as well as assisting wildlife officers in managing wild animals. The effectiveness of this method will be tested through field trials on animals. This project has the potential to contribute to wildlife conservation efforts and mitigate human-wildlife conflicts.

1.1 Proposed System

The proposed system for animal deterrence utilizes an ultrasonic sound generator. Unlike traditional methods such as electrified welded mesh fences, chemicals, or gas cannons, which can be cruel, ineffective, and environmentally polluting, the proposed method is based on animal-friendly ultrasound technology. The ultrasonic sound generated by the system does not cause physical or biological harm to animals, and is not audible to humans.

The ultrasonic sound produced by the generator creates perturbations in physiological and behavioral parameters of animals, such as heart rate, blood pressure, electroencephalographic changes, and seizing. These effects prompt animals to move away from the region where the ultrasonic sound is generated. The system operates within specific frequency ranges that are known to be audible to animals, as shown in Table 1.1, which displays the animal hearing spectrum ranges.

The advantages of the proposed system include its humane approach to animal deterrence, as it does not cause harm to animals or produce audible noise that may disturb humans. The system can be used to mitigate animal casualties resulting from road/railway accidents, protect crops from animal damage, and assist wildlife officers in managing wild animals.

LSU Deafness and Hearing Range. "Example of Animal Hearing Spectrum Ranges."

Sl.No	Animal	Approx Hearing range
1	Human	20Hz-22KHz
2	Dog	67Hz-45KHz
3	Cat	45Hz-64KHz
4	Horse	55Hz-33.5KHz
5	Sheep	100Hz-30KHz
6	Rabbit	360Hz-42KHz
7	Mouse	1000Hz-91KHz
8	Elephant	16Hz-12KHz
9	cheetah	30Hz- 64KHz
10	Tiger	20Hz-65KHz
11	Lion	24Hz-65KHz
12	Fox	20Hz-64KHz

Table 1.1: Animal hearing spectrum ranges

Source: <https://www.lsu.edu/deafness/HearingRange.html>

Field trials will be conducted to evaluate the effectiveness of the proposed system in deterring animals from specific areas. The results of these trials will be analyzed to determine the efficacy of the system and its potential for widespread implementation in wildlife conservation efforts and human-wildlife conflict mitigation. The proposed system presents a promising approach to addressing the increasing problem of animal casualties from road/railway accidents and crop damage caused by animals,

1.2 Organisation of Thesis

Chapter 1: Introduction

This chapter provides a brief overview of the need for a wildlife pathway alert system and discusses the disadvantages of current methods used to address this problem. It highlights the advantages of using an ultrasonic sound generator as a repellent to deter animals from sensitive areas such as roads, railways, and crops.

Chapter 2: System Architecture

This chapter provides an overview of the prototype of the project, including the selection of the ultrasonic speaker, moment/image detection methods, and powering methods. It discusses the design considerations and decisions made for the various components used in the system.

Chapter 3: System Simulation

This chapter explains the functional operation of the project using simulations. It includes discussions on the MPPT (Maximum Power Point Tracking) charge controller scheme and control topology. It also introduces the use of a DC-DC converter MOSFET's switch as an audio input instead of an additional amplifier for the ultrasonic speaker.

Chapter 4: Schematic and PCB Design

This chapter focuses on the schematic and PCB (Printed Circuit Board) design of the project using PCB design EDA software. It discusses practical aspects such as the selection of the micro-controller, switches, switching drivers, voltage/current measurement techniques, and other components used in the system.

Chapter 5: Testing

This chapter presents the results of testing the ultrasonic sound generator on animals. It discusses the effectiveness of the system in deterring animals from the device's location and presents data and analysis on the system's performance. It also discusses any ethical considerations and animal welfare measures taken during the testing process.

Chapter 6: Arduino Code Overview & Functionality

This chapter explores Arduino code for solar power management system , load voltage regulation using PID control, and battery charging management. It defines constants for system behavior, including PV parameters for MPPT and PID control. The code uses timers and PWM signals for battery charging and discharging. Overall, it efficiently manages solar power, load voltage, and battery charging through various functionalities and constants.

Chapter 7: Conclusion

This chapter provides a summary of the project and its findings. It highlights the advantages of using an ultrasonic sound generator as a deterrent for animals in various applications. It also suggests future research directions and recommendations for further improvement of the system.

Chapter 2

System Architecture

The system architecture of the ultrasonic sound generator for animal deterrence includes components such as an ultrasonic sound generator, battery, PV panel, output loads such as lights, control unit, and optional animal sensors. The PV panel charges the battery, providing power to the system, while the control unit regulates the battery charge control, operation of the ultrasonic sound generator, Output loads and Optional animal sensors.

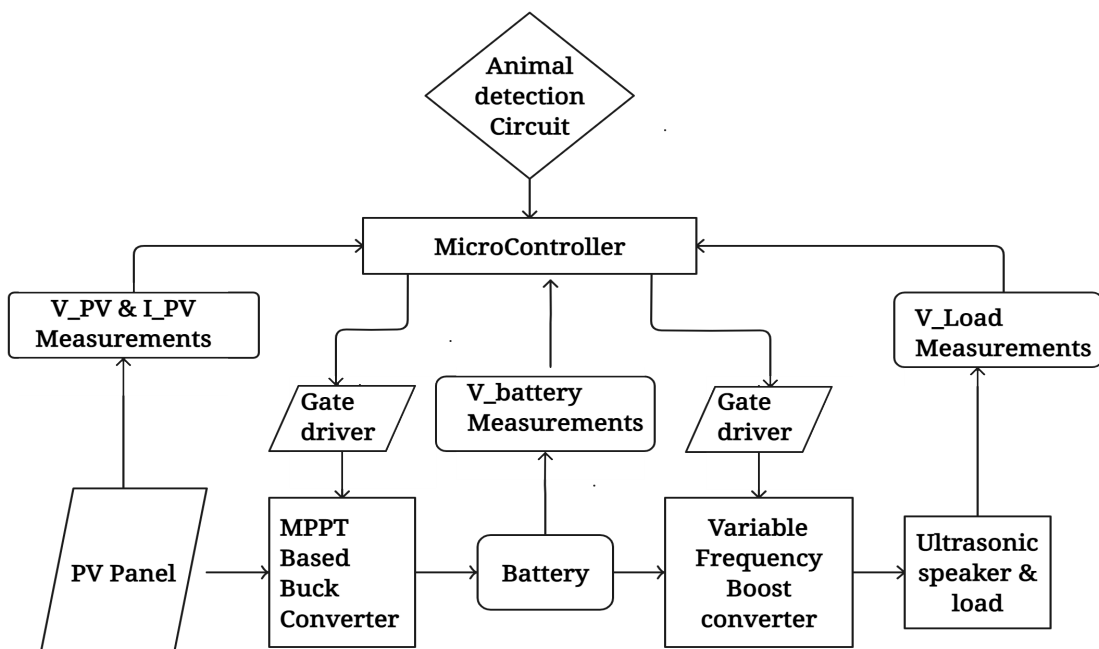


Figure 2.1: Proposed system architecture Block diagram

2.1 Powering the system

The system is powered by a solar panel in conjunction with an additional battery, which is charged by an MPPT charge controller to optimize solar panel performance and extract maximum power. For prototyping, a 12V lead acid battery is utilized. However, as the battery's voltage may fluctuate due to the state of charge (SoC), a DC-DC converter with closed-loop control is employed to ensure a consistent voltage at the load and ultrasonic speaker amplifier ends. This approach helps maintain the system's stability and efficiency.

2.2 Selection of ultrasonic speaker

Ultrasonic transducers are made from piezoelectric materials such as ceramic or quartz. These materials physically change shape when excited by an electrical pulse. These electrical pulses are switched on and off in rapid succession, which causes the piezoelectric materials to vibrate at high frequencies producing sound.

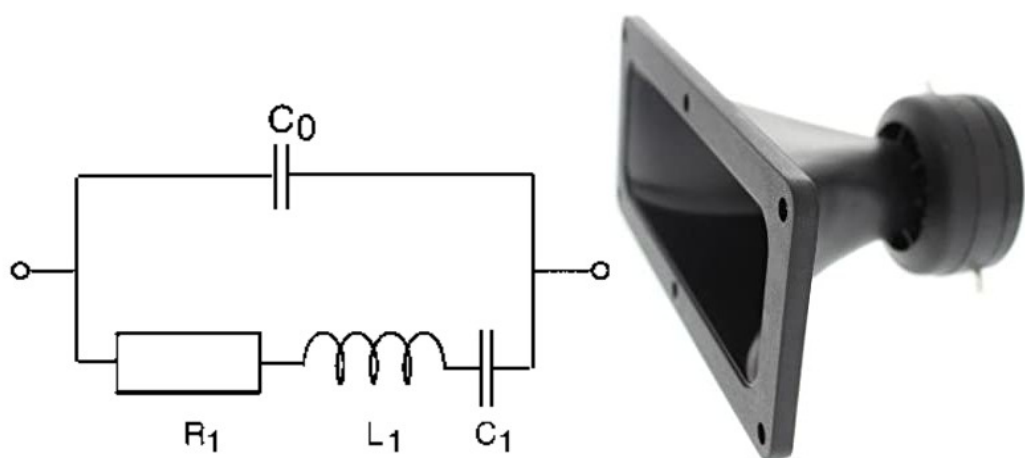


Figure 2.2: approx equivalent circuit and commercial Piezoelectric speaker

In order to test the working of the pizeo-electric speaker, an Arduino nano is used to create a variable frequency square wave and connected it to a mini pizeo electric

disc speaker and observed the sound spectrum in a mobile app to visualise the audio spectrum (since the max frequency supported by the phone internal sound card is 20KHZ, so tested for 10,15,20KHz)

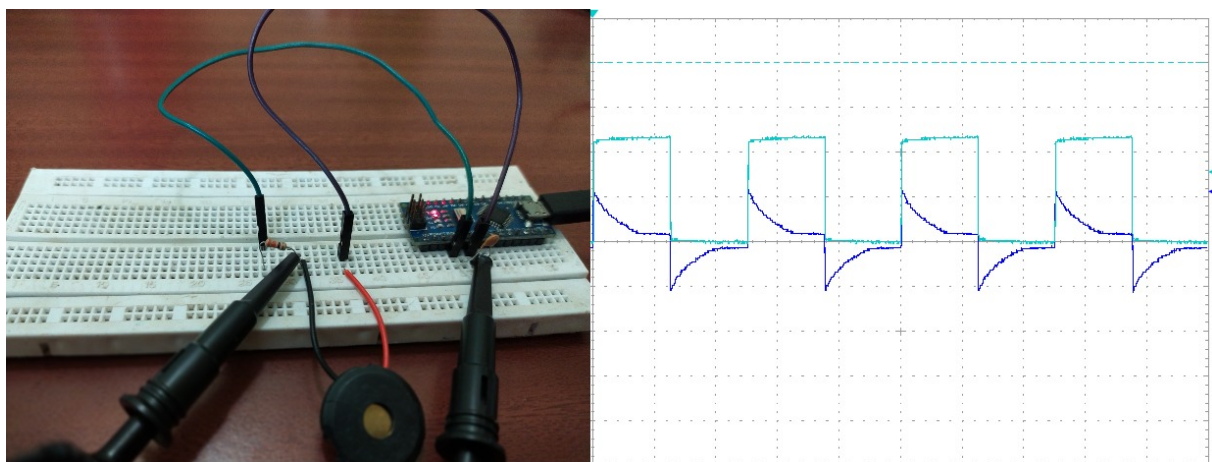


Figure 2.3: speaker Experimental setup, voltage applied(azure) and current drawn by speaker(Blue)

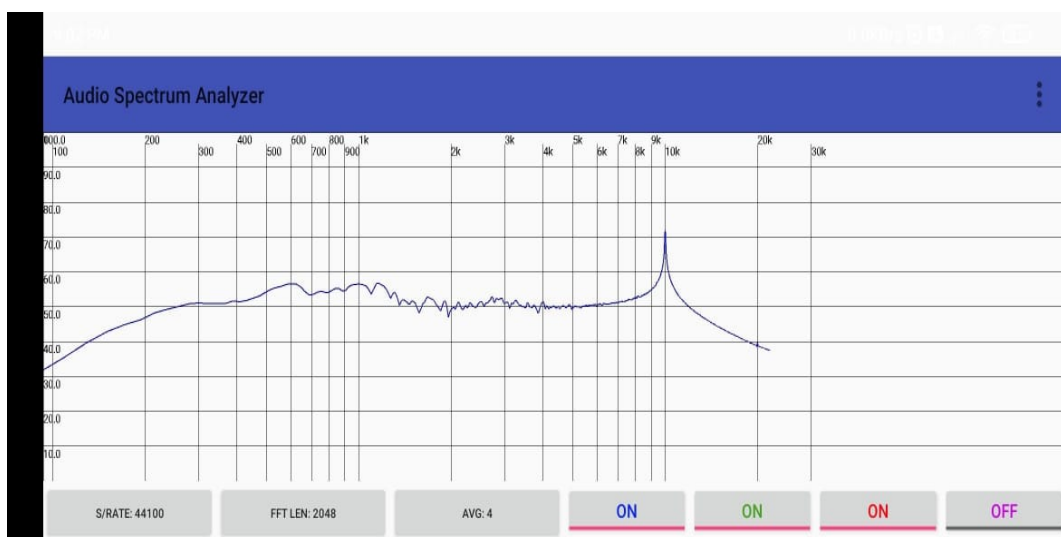


Figure 2.4: observed spectrum at 10KHz

2.3 Animal detection

In order to detect the animal, a motion detecting sensor needs to be used. the most common ones are

1) PIR Sensor 2) Microwave sensor 3) Hybrid 4) Image processing

1) Passive infrared (PIR) sensors use a pair of pyroelectric sensors to detect heat energy in the surrounding environment. These two sensors sit beside each other, and when the signal differential between the two sensors changes (if a animal/person enters, for example), the sensor will engage.

2)Microwave sensors also known as Radar, RF or doppler sensors are electronic devices capable of detecting motion from walking, running to crawling in an outdoor environment by using electro-magnetic radiation. It is able to detect motion by applying the Doppler effect and project microwaves which will bounce off surfaces and return to the sensor. It is able to measure and detect the amount of time for the signal to be reflected to the sensor which is known as echo time.

The advantage of the microwave sensor over the PIR is that it has 360° motion detection with a single sensor, consistent detection over all temperatures, and can sense movement through obstacles like trees. But the major disadvantage is that they can be triggered even by blowing leaves, moving branches, and other small objects, so the combination of PIR and microwave is used in the AND gate configuration, so it is called a hybrid motion detection sensor.

4)The major drawback of the above sensor is it not only detect the wild animals but also detects the movement of small birds and even human being. so an camera placed with image detecting algorithm. the major drawback of this setup is cost and it need more computational power. so in general the camera is turn on only after the PIR/microwave sensor is triggered to save power. (***Image processing was not tested in this project because it is outside the scope of the project*)

Chapter 3

System Simulation

3.1 Charging the battery

3.1.1 MPPT algorithm

PV array has non-linear I-V characteristic and output power depends on conditions such as solar irradiation and temperature. There is a point on I-V, P-V characteristic curve of PV array called as Maximum Power Point (MPP), where the PV system produces its maximum output power. The purpose of MPPT is to adjust the solar operating voltage close to MPP under changing environmental conditions. In order to continuously gather the maximum power from the PV array, they have to operate at their MPPT despite of the in-homogeneous change in environmental conditions. The most commonly used algorithm for low-power PV applications, due to its ease of implementation, is Perturb and Observe (P&O). MPPT algorithm, which can be implemented in software or embedded in the controller of the PV system to adjust the operating voltage and track the MPP.

Current-Voltage & Power-Voltage Curve (250S-20)

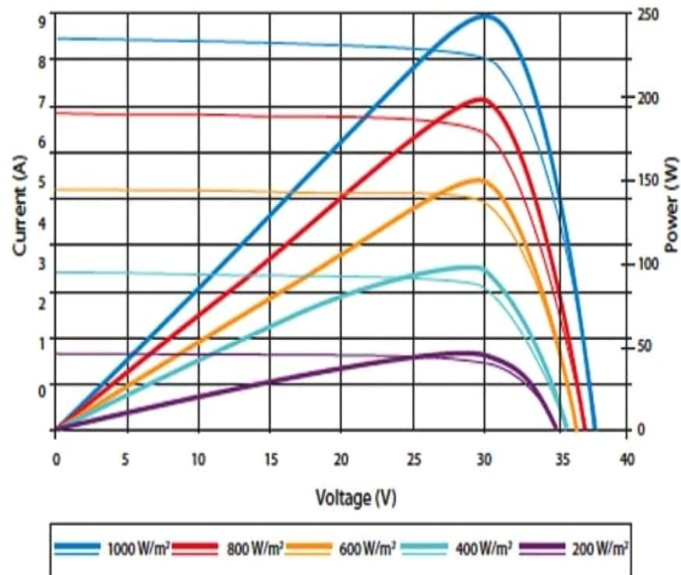


Figure 3.1: Voltage, Current and power curve for a PV

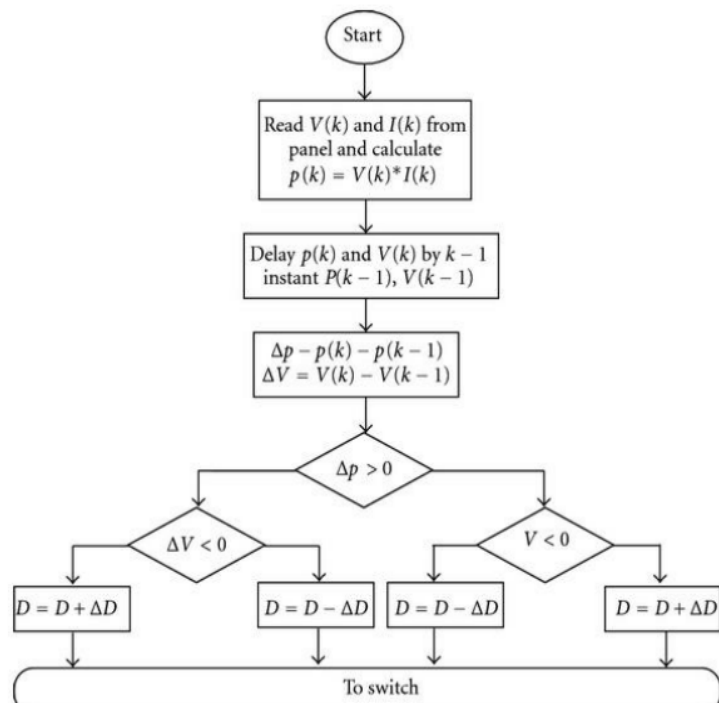


Figure 3.2: P/O algorithm for MPP Operation

3.1.2 Simulating MPPT Buck converter

for the simulation a PV panel with MPPV & MPPC of 19.25V & 1.06A respectively taken which gives 20.4 watt max-power respectively at 1000W/m²

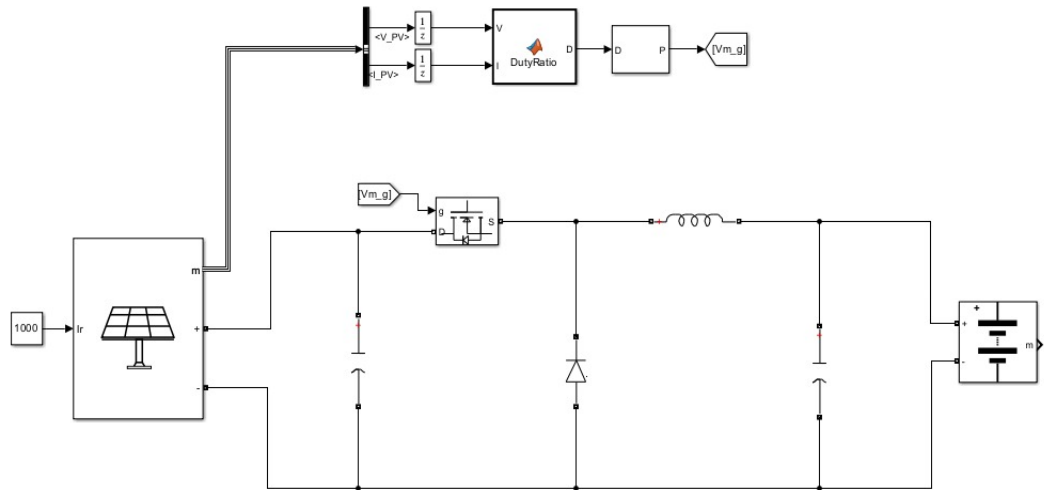


Figure 3.3: Simulation of MPPT charge controller

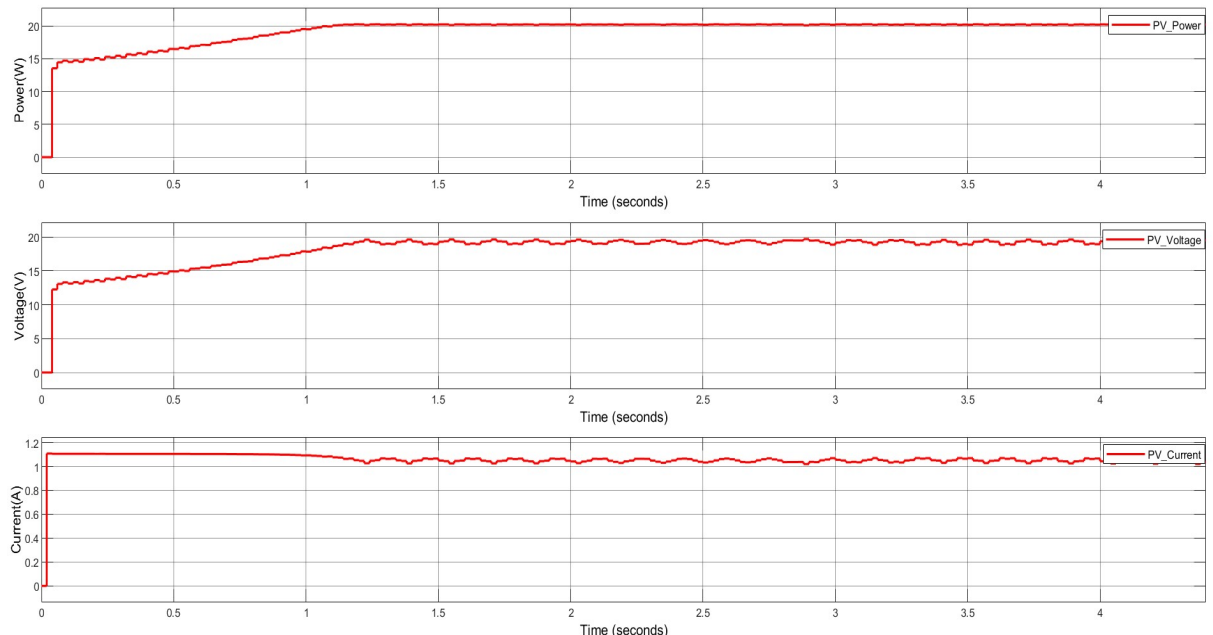


Figure 3.4: Voltage, current, and power output Vs Time of PV @1000W/m²

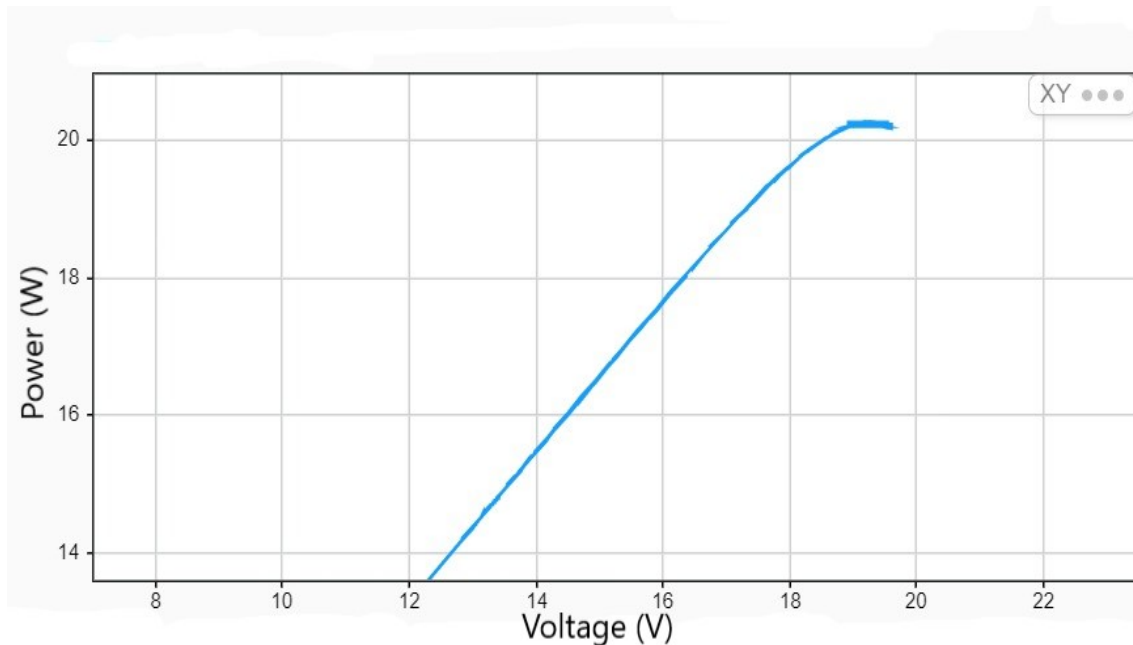


Figure 3.5: power Vs Voltage of PV @1000W/m²

3.2 Powering Load & speaker

3.2.1 Boost converter switch as amplifier

A DC-DC converter with a closed-loop system is used to provide a stable voltage for powering lights and ultrasonic speakers, as the battery voltage varies due to battery State of Charge (SOC). Instead of using a separate amplifier, the switch in the DC-DC converter can be utilized as an amplifier by changing the switching frequency, allowing for the creation of ultrasonic sound of different frequencies. This way, an amplifier and a boost converter can be integrated into a single circuit, as shown below.

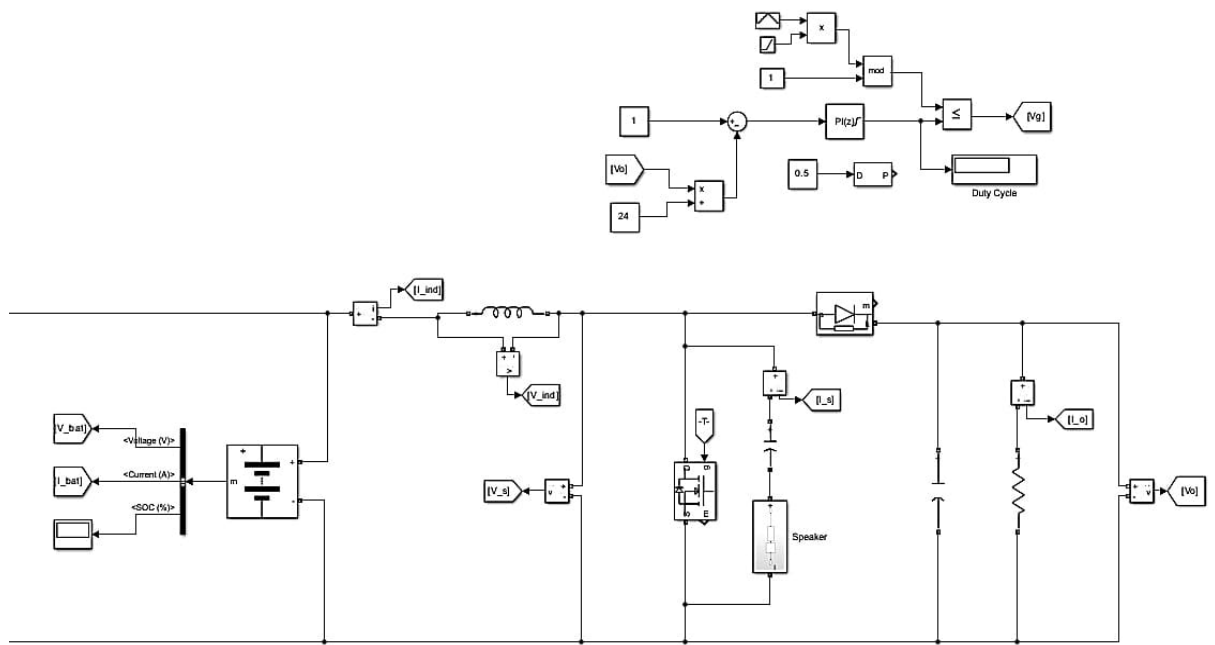


Figure 3.6: Boost converter with speaker connected ac cross switch

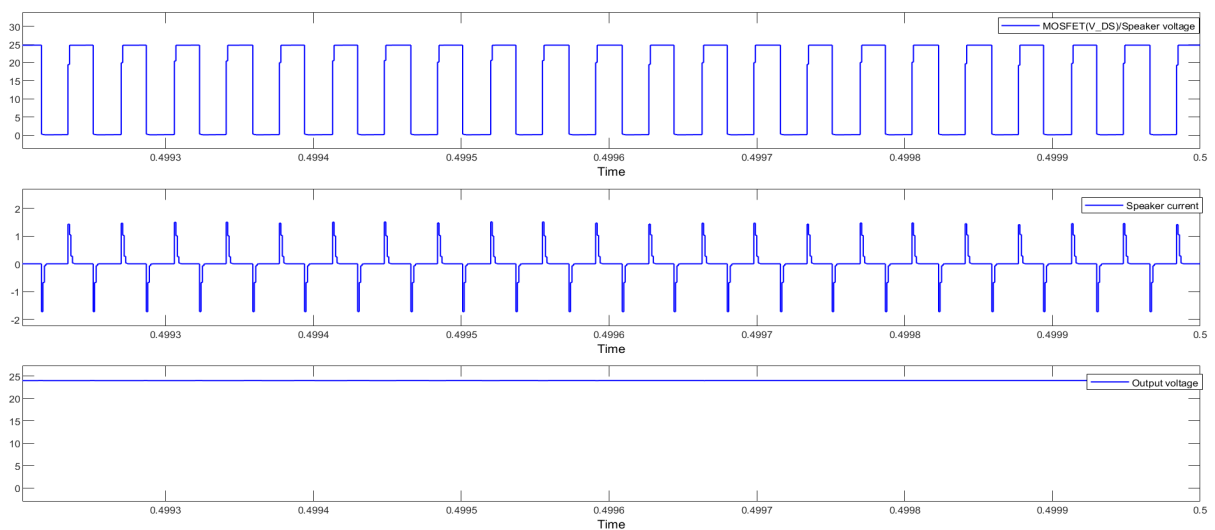


Figure 3.7: Speaker voltage, Currents & Load Voltage Vs Time

3.3 BMS & Load Shortcircuit Protection

In order to ensure the normal operation of charging and discharging, as well as prolong the service life of a lead-acid battery, a battery management system (BMS) must be implemented. The BMS monitors various battery indices to prevent overcharging and overdischarging. Specifically, in the case of a solar charge controller, it should automatically switch from Maximum Power Point Tracking (MPPT) mode to constant voltage mode when the battery bus voltage reaches 13.5V to prevent overcharging. Additionally, the battery should be disconnected from the load when the voltage drops below 11.5V to prevent overdischarging, and the DC-DC converter should be turned off at low voltage. It's also important to include reverse voltage protection features using diodes and fuses, blocking current flow in the wrong direction and providing safety against potential damage from reversed polarity and the use of PPTC fuses in the load output circuitry offers superior performance compared to conventional fuses, ensuring reliable operation even under challenging conditions, and providing efficient short circuit protection for enhanced safety and longevity. With PPTC fuses, the system enjoys increased stability, reduced downtime, and improved overall performance, making it a preferred choice for critical load applications.

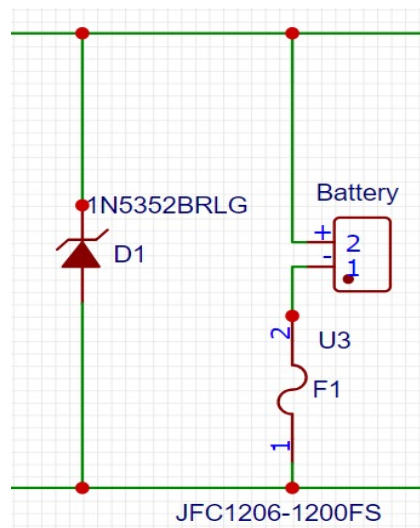


Figure 3.8: Battery Over-voltage,Over-current, Reverse voltage protection by a Fuse and High-power Zener diode

Chapter 4

Circuit Design

4.1 Description of Microcontroller

MPPT Algorithm, Switching of MOSFETs, closed loop feedback controls, battery charge control, etc., need to be controlled in this project. However, designing analog logic circuits to control all these parameters is not within the scope of this project, as it can be expensive and the parameters cannot be easily changed once installed. A better solution is to use a microcontroller for system control.

A microcontroller (MCU) is the smallest and most basic computer that runs on a single chip, consisting of a CPU, RAM, ROM, and input/output ports. Unlike a microprocessor, which serves more generalized applications, a microcontroller is designed for more specific applications. Therefore, it is essential to choose a microcontroller that is most appropriate for the project, taking into consideration factors such as hardware architecture, memory, hardware interface, software architecture, and cost.

Arduino Nano is chosen as the microcontroller for this project due to its low cost, low power consumption, and user-friendly IDE (Integrated Development Environment). It comes with an inbuilt USB to UART converter, making it easy to program the microcontroller (Atmega328p) using USB.

4.1.1 Arduino Nano

The following image shows the layout of a typical Arduino nano board.

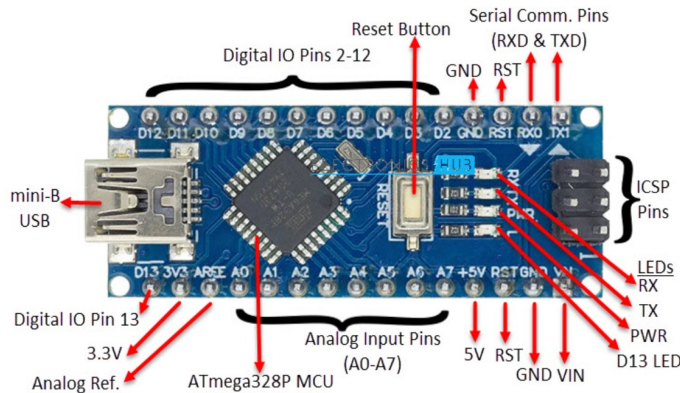


Figure 4.1: Layout of Arduino Nano Board Top view

4.1.2 Technical Specifications of Arduino Nano

As Arduino Nano is also based on ATmega328P Microcontroller, the technical specifications are

Microcontroller	ATmega328P (SMD)
Operating Voltage	5V
Input Voltage	6V-20V
Digital I/O Pins	14 (6 PWM)
Analog I/O Pins	8
Max Current Per I/O	40mA
Flash Memory	32KB (2KB Used by Bootloader)
SRAM	2KB
EPROM	1KB
Clock	16MHz
Dimensions	45mm x 18.5mm
Weight	7g

Table 4.1: Technical specifications of Arduino Nano

4.1.3 Input and Output Pins of Arduino Nano

The Arduino Nano board has a total of 30 pins, out of which 22 pins are associated with input and output. Among these, 14 pins (D0 to D13) are true digital IO pins that can

be configured as per the application using `pinMode()`, `digitalWrite()`, and `digitalRead()` functions. These digital IO pins are capable of sourcing or sinking 40mA of current. Additionally, the digital IO pins 3, 5, 6, 9, 10, and 11 are capable of producing 8-bit PWM signals, which can be used for controlling Duty-cycle.

The Nano board also has 8 analog input pins (A0 to A7) that provide a 10-bit resolution ADC feature, which can be read using the `analogRead()` function. These pins can also be configured as digital IO pins, except for A6 and A7.

Furthermore, the Nano board supports three different types of communication interfaces - Serial, I2C, and SPI. The digital IO pins 0 and 1 are used as Serial RX and TX pins for serial communication and are connected to the on-board USB to Serial Converter IC, which is used for programming the Arduino board.

Analog input pins A4 and A5 have alternative functions and can be configured as SDA (A4) and SCK (A5) to support I2C or Two Wire Interface (TWI) communication. Lastly, digital IO pins 10, 11, 12, and 13 can be configured as SPI pins for SS, MOSI, MISO, and SCK respectively, to enable SPI communication.

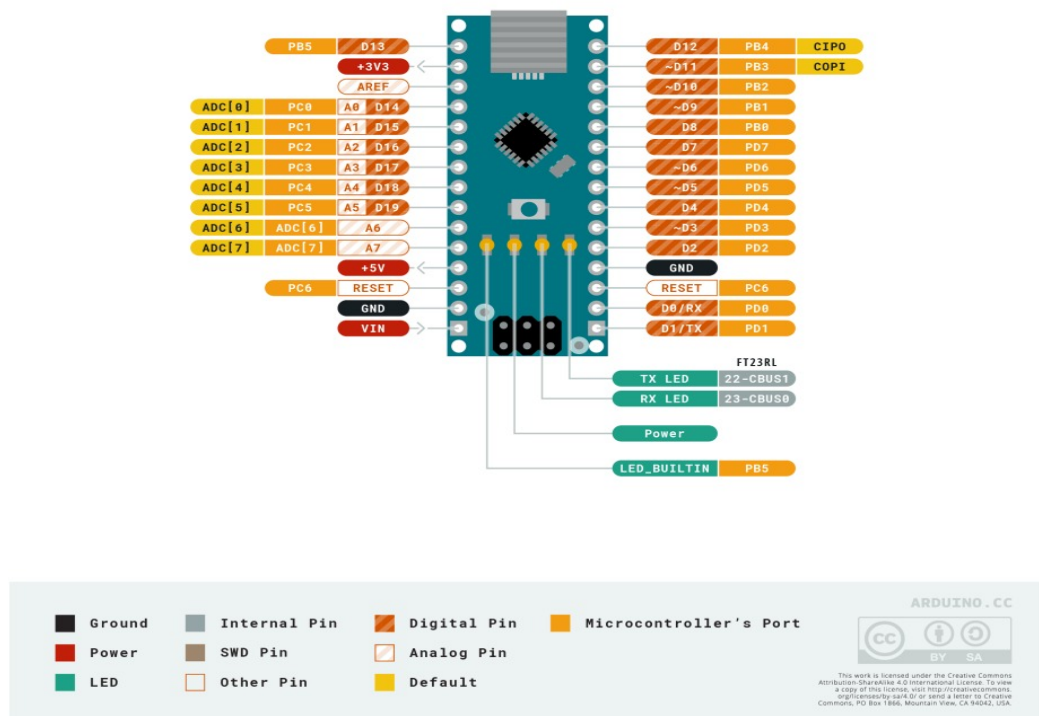


Figure 4.2: Power Tree of Arduino Nano (image taken from arduino usermanual)

4.1.4 Powering the Arduino Nano

There are a couple of ways in which arduino nano can be powered. The first and easy way is using the mini-B type USB Connector which is not possible in the project.the next alternative is to use an onboard regulator at the bottom (along with the USB – to – Serial Converter). To use, we can provide an unregulated supply in the range of 6V to 20V to VIN pin of the Nano (Pin number 30). but this method heats the board a lot and inefficient for example the battery used here are lead acid battery with nominal voltage of 12V so the efficiency will be around 40% so 5V regulated external power supply (pin 27) is used. in this project I am using mp2307 ic based on synchronous buck converter wide range of input voltage (upto 28V) and maintains the constant voltage irrespective of load upto max current of 2A.

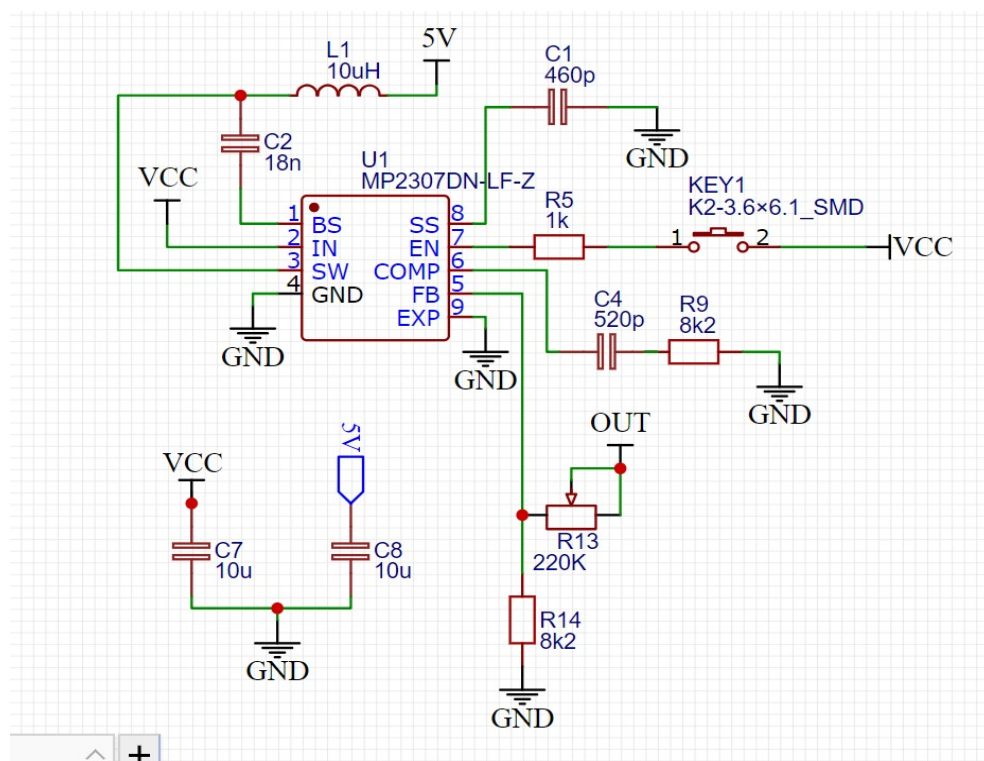


Figure 4.3: Schematic for mp2307

4.2 Voltage and Current Measurement

In the Simulink for the PV,battery voltages are measured using voltage,current measurement blocks for MPP and charge control operations but in practical situation it is required to design an voltage and current sensors such that Micro-Controller can reads the analog data from the ADC channel and do the control operations. this subsection describes how the voltage and current measurement is done.

4.2.1 Voltage measurement

The Magnitude of voltage needs to measure in this project is 24V(PV) & 12(Battery) so directly connecting the pin to Arduino kills the ADC channel since the max ADC voltage of ATmega 328p is 5.5V so a voltage divider is used in such a way that max voltage at input of analog input pin cannot go beyond 5V thus the schematic represents the voltage measurement using the voltage divider technique

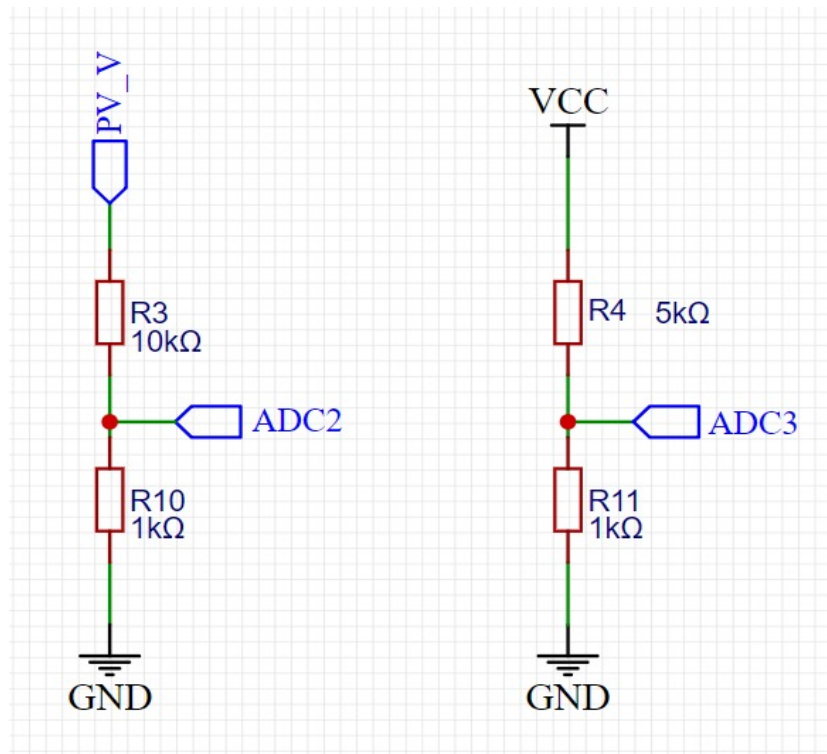


Figure 4.4: Schematic for voltage measurement using Resistive divider Technique

4.2.2 Current measurement

In general the DC current measurement can be done by using hall-effect sensor or series Resistance voltage drop method.

A hall effect current sensor works based on conductor produces a magnetic field comparable to the current. The magnetic field is concentrated by the core and measured by the Hall sensor. The signal from the Hall generator is low, so it is amplified, and it is this amplified signal that becomes the sensor's output. generally hall effect used for large value of currents

A Series Resistance based current measurement is based on the Ohms law. voltage accross the a fixed resistance is proportional to the current flown through the resister so by using this property current can can be converted to voltage. in general the small series resistance taken. so the voltage produced across the resistance is very very small so amplification is needed.

In this project the Series Resistance based current measurement is used since the current rating is small and it is cheap when compared to hall effect sensor. the voltage amplification here is done by using an inverting amplifier and connected to ADC of Microcontroller.

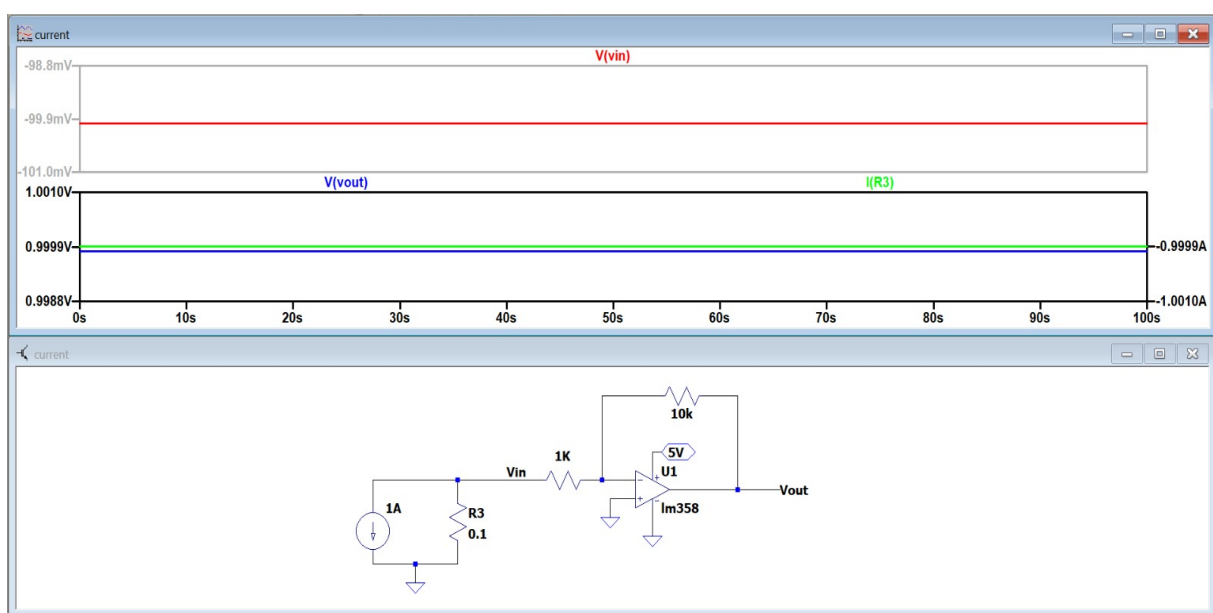


Figure 4.5: Simulation for Current Measurement

4.3 Power Inductor and Capacitor Selection

4.3.1 Power Inductor Selection

The Value of the Inductor in the MPPT Buck & Boost converter is selected based on the ripple current. With the Smaller inductor, the current ripple in the inductor will be higher thus large filtering Capacitor and core with a high saturating limit are required and with the large value of the inductor the ripple current will be lowered but the overall size and resistance increase. Thus a trade-off is maintained.

4.3.2 Capacitor selection

The selection of capacitors for a project is crucial and depends on various factors such as ripple current, ripple voltage, and performance requirements. Electrolytic capacitors are often chosen for their high capacitance x voltage (CV) rating and low equivalent series resistance (ESR), making them suitable for energy storage applications, where a large capacitance is required in a compact size. On the other hand, ceramic capacitors are commonly used for their small size, high capacitance values, and low cost, making them ideal for high-frequency filtering and decoupling purposes. Both types of capacitors can play important roles in a project, with electrolytic capacitors providing energy storage capabilities and ceramic capacitors providing high-frequency filtering and decoupling, ensuring stable and reliable operation of the circuit. Careful consideration of the specific requirements and characteristics of different capacitor types is essential for optimal performance and reliability in the final design.

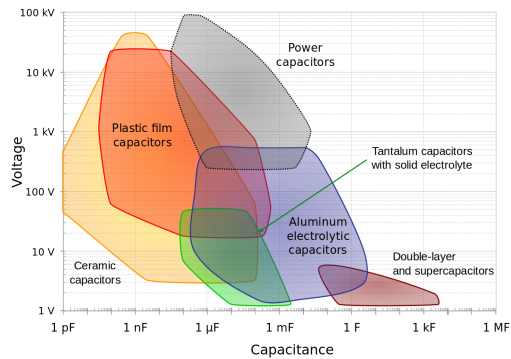


Figure 4.6: Capacitor types and ranges

4.4 Converters Design Considerations

4.4.1 Selection of Power Switches & Diodes

When selecting power electronic switches and diodes for a project, several parameters should be considered for optimal performance:

- **Conduction losses:** This refers to the product of the current and voltage across the device while it is conducting. For a BJT, this will depend on V_{ceSat} , while for a MOSFET, it's about R_{dsON} .
- **Switching losses:** These losses depend on the switching speed, which is influenced by the gate to drain/source capacitance and stored charge for BJTs.
- **Driving losses:** This refers to the amount of base/gate current required to drive the device.
- **Simplicity and requirements:** Consider the driving circuit's complexity, especially in terms of PMOS versus NMOS switches. For example, a high-side NMOS switch may require a bootstrap capacitor or a charge pump to stay on continuously, while a PMOS switch does not, but may have lower efficiency.
- **Cost:** Cost should not be limited to just the component's initial price. A more expensive component that offers better efficiency may be more cost-effective in the long run, as it may not require additional expenses such as a heat sink.

By considering these parameters, the selection of power switches and diodes can be optimized for the specific requirements of the project.

The power electronic converters used in this project operate at higher frequencies (10kHz - 100kHz). MOSFETs are chosen as switches due to their lower voltage drop when turned on compared to BJTs, as well as their simpler and more efficient driver design. For diode selection, Schottky diodes are used due to their lower voltage drop

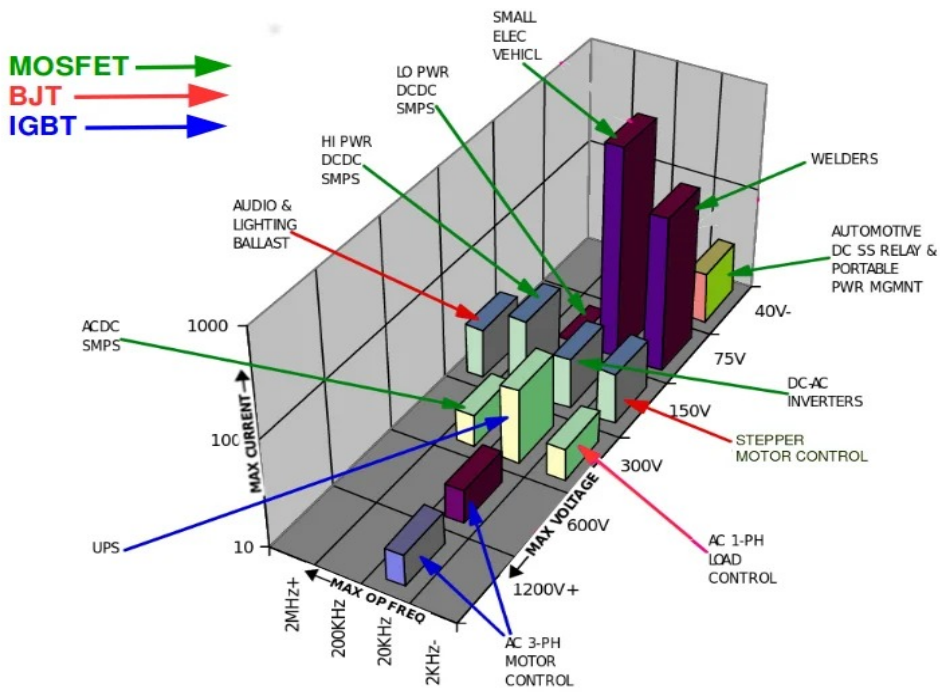


Figure 4.7: Three Dimensions of Power Transistor Applications

under forward bias, fast recovery time, and low energy loss at higher frequencies. Alternatively, a second MOSFET may be used instead of a Schottky diode, which would normally be switched on and off in a complementary fashion to the first MOSFET, referred to as "synchronous" operation. However, since the project deals with very low amperes, synchronous operation is not required.

4.4.2 Need for MOSFET Gate driver

In general MOSFET's have very low gate capacitance. For example, the IRFZ44N from International Rectifier has 360pF of input capacitance. Ideally the Gate of the mosfet doesn't require any current to make MOSFET conducting but with increase in the switching frequency it required to charge and discharge the Gate capacitance of the MOSFET at faster rate since For lowest ON resistance you would want to drive the gate as high as possible, say 15V and to minimise power dissipation you want to switch quickly between ON and OFF and vice versa otherwise the transistor will spend a relatively long time in the saturation region rather than the linear or ohmic region. The gate current may be several times higher (as shown in below simulation) than what a micro controller can provide so to prevent the destruction of Micro-controller by overloading its digital pin a driver is used between micro-controller and Gate of MOSFET's. other features of Gate drivers are

Voltage level translation: MOSFETs typically require a gate-source voltage (V_{gs}) higher than the logic level voltage (e.g., 5V or 3.3V) used in most control circuits. A MOSFET driver can provide the necessary voltage level translation to ensure proper turn-on and turn-off of the MOSFET.

Gate charge management: MOSFETs have a capacitance between the gate and source terminals, known as gate charge (Q_g). The gate charge needs to be charged and discharged quickly to achieve fast switching speeds and reduce switching losses. MOSFET drivers are designed to efficiently manage the gate charge, ensuring rapid switching and optimal performance.

Protection features: MOSFET drivers often include protection features such as over-voltage protection, over-current protection, and short-circuit protection. These features help to safeguard the MOSFET and the overall circuit from potential damage due to abnormal operating conditions.

4.5 Converters Design

4.5.1 Boost Converter

The Boost Converter is used to power the load and Speaker from battery. Circuit is designed on Pref board PCB as Schematic diagram shown below. boost converter is tested with $V_{in} = 12V$, V_{out} set to 20V and switching frequency of 32Khz by connecting ultrasonic speaker across the drain and source of the MOSFET

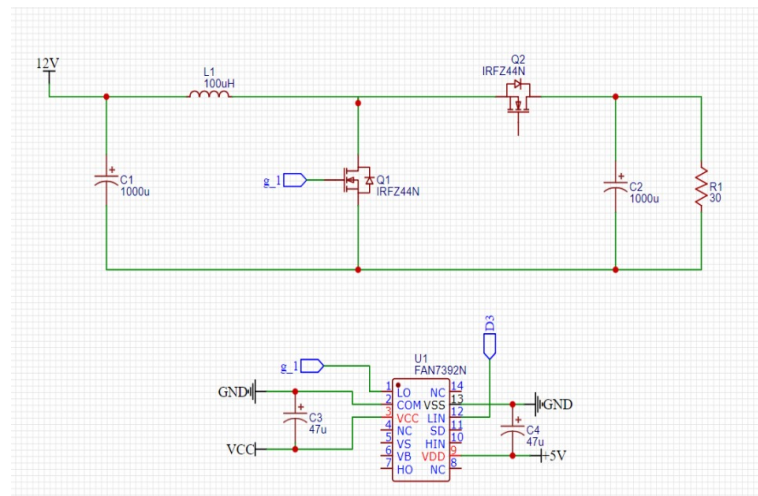


Figure 4.8: Boost Converter Circuit Schematic

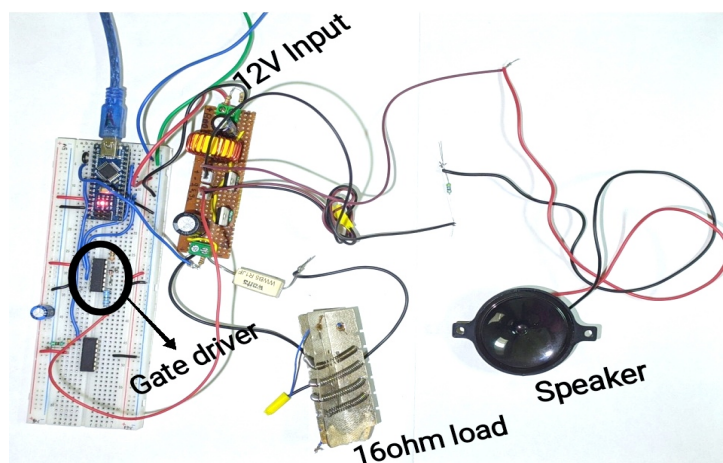
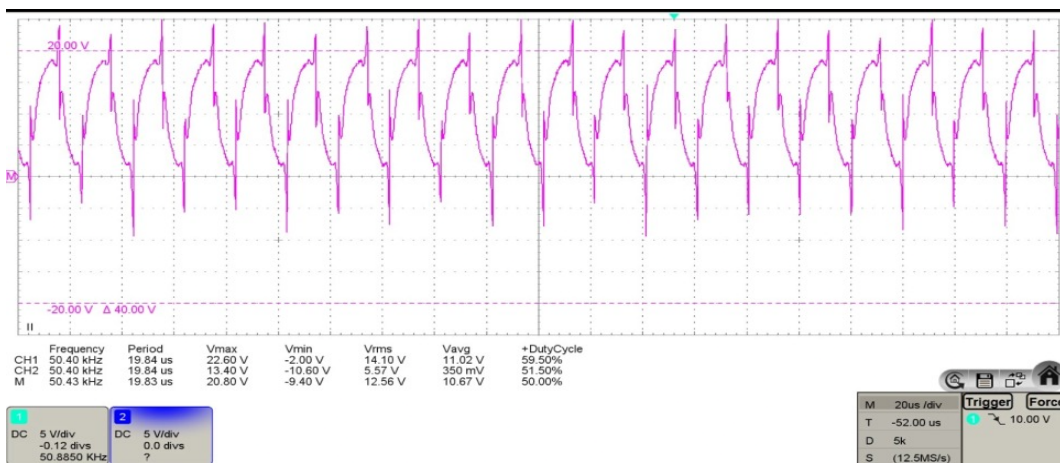
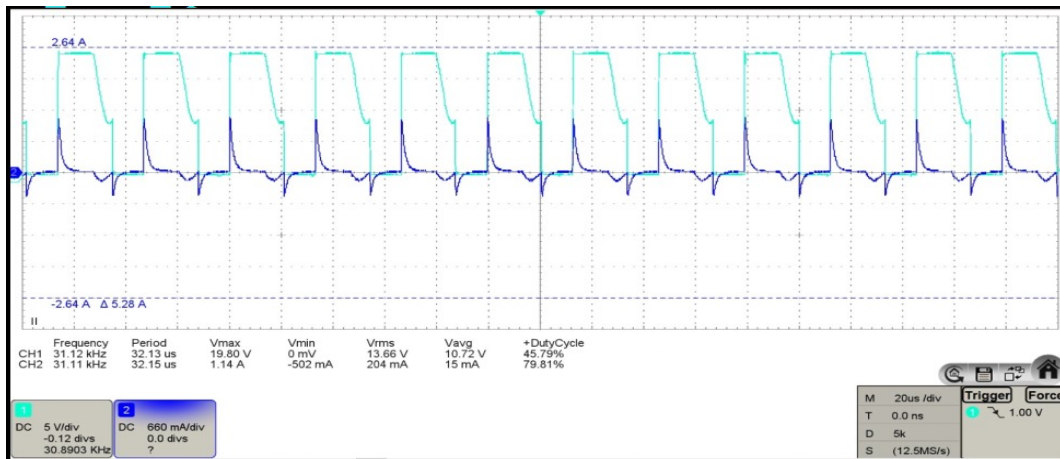


Figure 4.9: Boost Converter Circuit Test Setup



4.5.2 Buck Converter

The Buck Converter is used here to charge a battery from a PV panel. In a Buck converter, MOSFET is connected between PV(+) and the inductor, and the switch Node point at the inductor is floating. To ensure proper operation of the MOSFET with a perfect gate signal across V_{GS} , which is not possible in this case, bootstrapping is used to trigger the on/off state of the MOSFET. the MOSFET is used to control the flow of current through the inductor, which regulates the output voltage. However, in some cases, the switch point at the inductor can be floating, meaning it is not connected to a fixed voltage reference. This can make it challenging to drive the MOSFET with a proper gate signal, as the gate voltage needs to be higher than the source voltage for

the MOSFET to turn on fully.

To overcome this challenge, bootstrapping is used. Bootstrapping is a technique where a capacitor is connected between the high-side (PV side) of the MOSFET and its gate. During the switching operation, when the MOSFET is turned off, the capacitor charges up to the high-side voltage, effectively providing a higher gate voltage for the MOSFET during the next switching cycle. This allows the MOSFET to fully turn on and off, ensuring efficient operation of the Buck converter. Bootstrapping is a common technique used in Buck converters to ensure proper gate drive for the high-side MOSFET when the switch point at the inductor is floating.

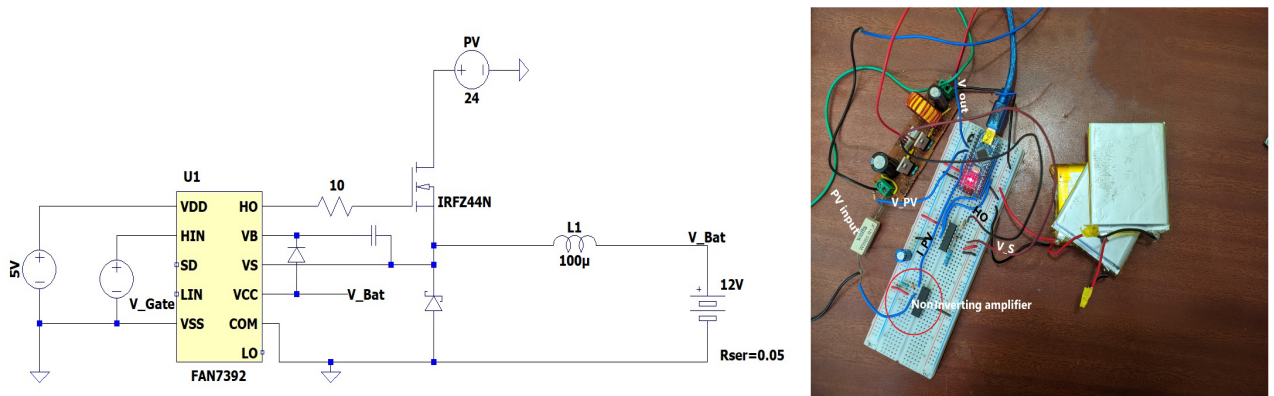


Figure 4.12: Schematic Diagram and Experimental Setup for Buck converter by Bootstrapping

After testing the above Buck converter circuit, it was observed that the switching of the MOSFET was unable to start due to the absence of pre-charge in the bootstrapping capacitor. In normal bootstrapping operation, the capacitor is pre-charged from the source via a bootstrapping diode. However, in this case, the load is a battery and the load voltage and V_{CC} of the gate driver are the same, resulting in the voltage across the capacitor being "0". As a result, there is no pre-charge and the bootstrapping process does not start.

To solve the above issue the following methods can be Implemented

1) Use an external voltage source for bootstrapping: One solution is to use an external voltage source to pre-charge the bootstrapping capacitor independently of the load voltage. This can be achieved by connecting a separate voltage source, such as a charge pump or a dedicated bootstrap capacitor charging circuit, to charge the bootstrapping capacitor during the off-time of the MOSFET. This ensures that the bootstrapping capacitor is adequately charged before the MOSFET starts switching.

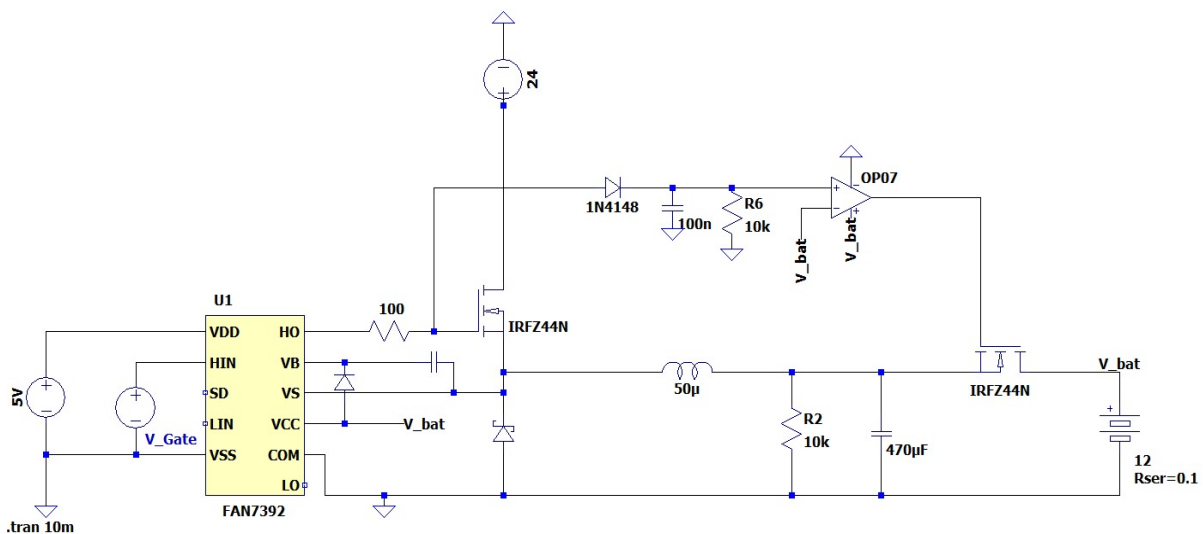


Figure 4.13: Simulation Schematic Diagram for Bootstrapping Pre-charge Circuit

The circuit shown above is a modified bootstrapping circuit where a MOSFET is used to disconnect the battery when the voltage across the bootstrapping capacitor is not sufficient to start the bootstrapping operation. This allows the capacitor to charge through a $10K\Omega$ resistor, enabling the bootstrapping operation to commence. Once the capacitor is adequately charged, the MOSFET is turned on, allowing the buck converter operation to start.

Merit : Works at all operating conditions and makes use of FAN7392 driver, which is used for boost operation. Thus, a single driver can be utilized for both high-side and low-side switching, reducing the additional driver cost.

deMerit : An additional MOSFET and the corresponding gate triggering circuit are necessary, which results in increased space and cost requirements for the project.

2) Use a dedicated voltage regulator for gate driver: Another solution is to use a dedicated voltage regulator to generate the gate driver's supply voltage (VCC) that is independent of the load voltage. This can provide a stable and regulated voltage for the gate driver, ensuring that the bootstrapping capacitor is pre-charged properly, regardless of the load voltage.

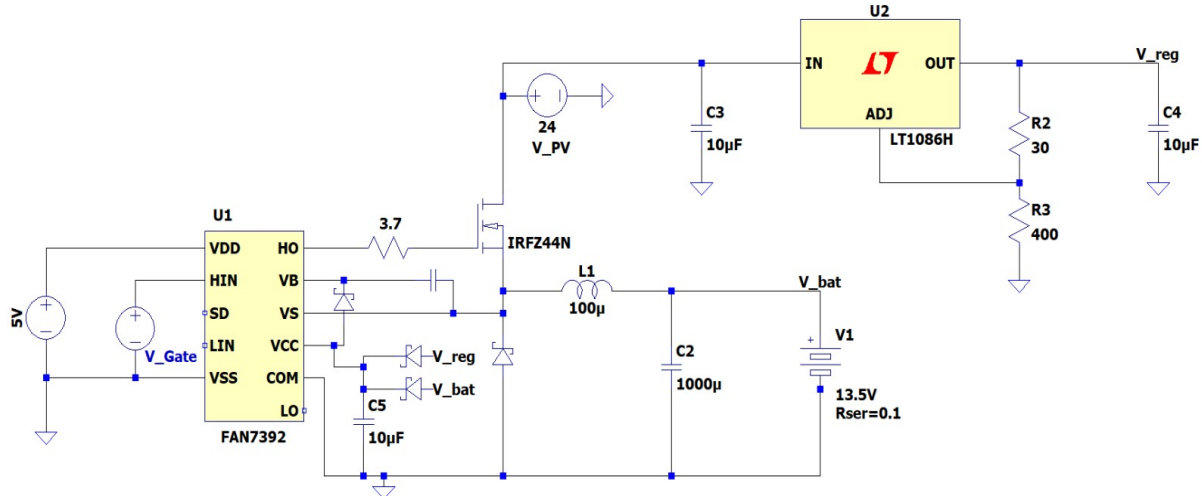


Figure 4.14: Schematic for Bootstrapping operation by using voltage regulator

In the above circuit, an external higher voltage source (PV panel) is used to power the gate driver, and a low dropout voltage (LDO) regulator is added in series to prevent damage to the FAN7392, as its maximum VCC is 20V. The parallel diode configuration in the circuit is implemented because the boost converter shares the same FAN7392 driver. During night-time or when the PV_{reg} voltage is low, the gate driver is powered by the battery to ensure the proper operation of the boost converter.

Merit : Makes use of FAN7392 driver, which is used for boost operation. Thus, a single driver can be utilized for both high-side and low-side switching, reducing the additional driver cost.

deMerit : Bootstrapping Operation may not work at lower input PV voltages.

3) Transformer-coupled gate drive topology:

A pulse transformer is a type of transformer specifically designed for transferring pulses of energy while providing electrical isolation. In the context of the project, the primary winding of the pulse transformer is connected to the FAN7392 driver, while the secondary winding is connected to the gate and floating source terminal of the high-side MOSFET. When the control circuitry generates a gate drive signal, a voltage pulse is applied to the primary winding, inducing a corresponding voltage in the secondary winding, which then turns the MOSFET on or off as required. The galvanic isolation provided by the pulse transformer ensures electrical isolation between the control circuitry and the high-voltage side of the buck converter, ensuring safety and noise immunity.

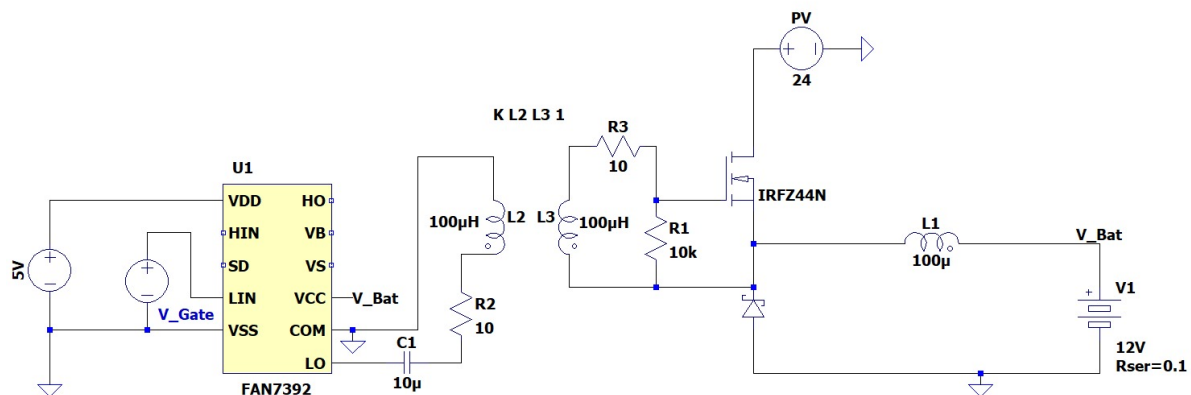


Figure 4.15: Simulation Schematic Diagram for Transformer-coupled gate driver

Merit : Makes use of FAN7392 driver, which is used for boost operation. Thus, a single driver can be utilized for both high-side and low-side switching, reducing the additional driver cost.

deMerit : Ideal transformer models used in simulation tools do not capture the non-ideal characteristics of real-world transformers, such as winding resistance, leakage inductance, and core losses, which may impact the accuracy of simulation results. Pulse transformers can add additional cost to the overall circuit additionally introduce additional losses in the form of winding resistance, leakage inductance, and core losses, which can impact the overall efficiency of the converter circuit.

4)an isolated Power Supply for Gate driver.

an isolated power supply can be used for the gate driver in the above circuit, it would provide a separate and isolated power source for the gate driver, independent of the rest of the circuitry.

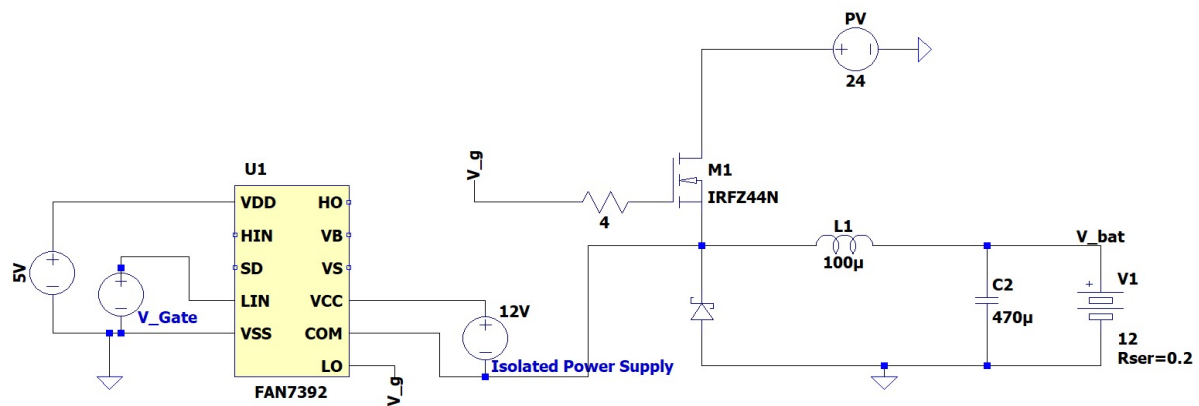


Figure 4.16: Schematic Diagram for Gate driver driven by isolated Power Supply

Merit : Works at all operating conditions

deMerit : Separate Gate driver is required for Boost and Buck converter as switch in Boost converter is low side which make the Gate driver non-isolated if same Gate driver is used. Isolated power supplies may be more expensive compared to non-isolated power supplies, which could add additional cost to the overall circuit and additional space and weight in the circuit layout.

5) BJT based Buck converter .

a PNP BJT is used as the main switch, the drive circuitry would need to be designed to accommodate the characteristics of a BJT, such as the base-emitter voltage (V_{be}) requirements. This can be easily implemented by a NPN Transistor as base drive circuit as shown in figure

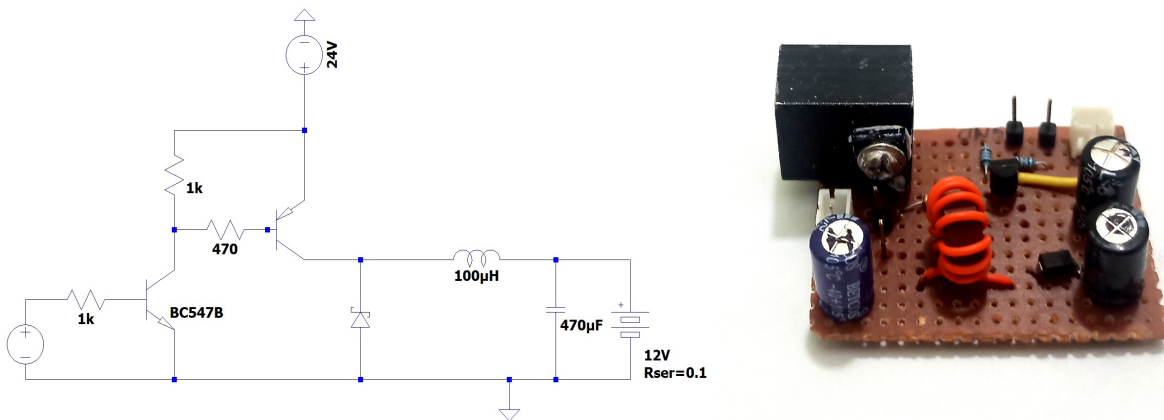


Figure 4.17: Schematic Diagram for BJT based Buck converter and Designed Circuit

Merit : External Gate driver is not required and BJTs are generally cheaper compared to MOSFETs, which could result in cost & Space savings in the overall circuit.

deMerit :

i) Higher voltage drop: PNP BJTs typically have a higher voltage drop compared to MOSFETs (0.5V in my case), which could result in lower efficiency in the circuit.

ii) Heat dissipation: Due to the higher voltage drop and potentially higher power dissipation, BJTs may require additional heat sinking or cooling measures to prevent overheating, which could add to the complexity and cost of the design.

6) P Channel MOSFET as High side Switch . In the buck converter where a P-channel MOSFET is used to drive a battery as the load and a photovoltaic (PV) panel as the input, a common gate driver with complementary output can be used, depending on the specific requirements and design considerations. However, it is important to ensure that the gate-to-source voltage ($|V_{GS}|$) of the P-channel MOSFET is pulsed between 0 and a magnitude greater than the threshold voltage ($|V_{th}|$), but lower than the maximum gate-source voltage ($|V_{GSmax}|$) of the MOSFET. This ensures that the gate voltage (V_G) of the P-channel MOSFET is pulsed between V_{PV} and a value less than ($V_{th} - V_{PV}$), and lower than the maximum gate-source voltage ($|V_{GSmax}|$) of the MOSFET. If a common gate driver with complementary output is used, it may limit the max input PV voltage due to the maximum gate voltage of the MOSFET to ensure proper operation and avoid damaging the MOSFET. thus to solve this issue a Gate voltage level shifter circuit is designed as shown below

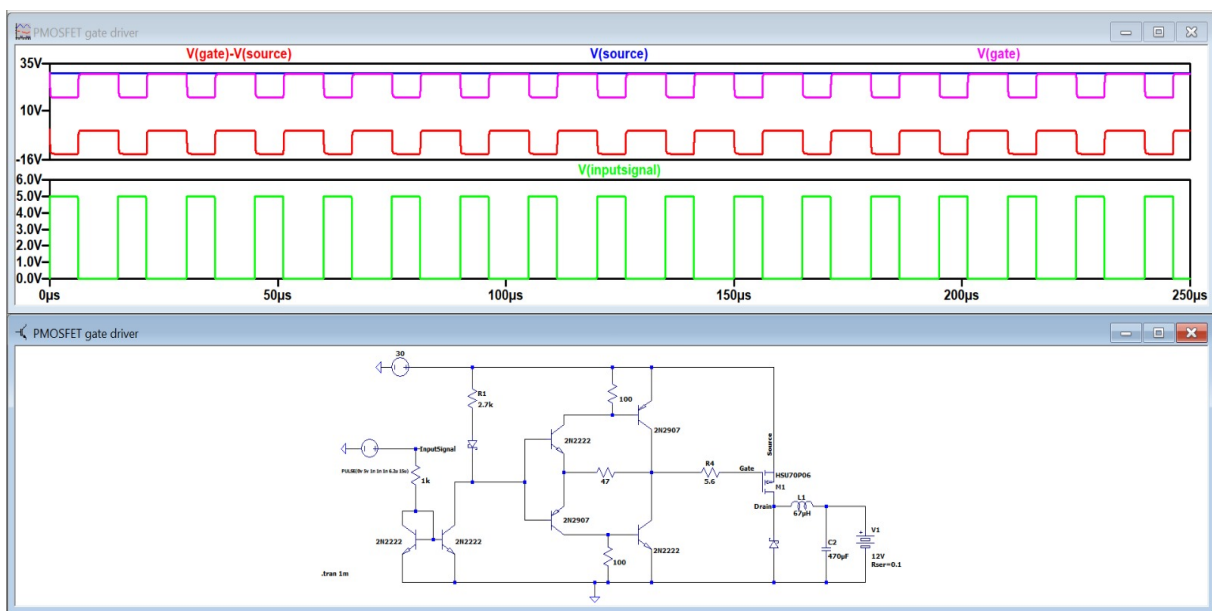


Figure 4.18: Gate driver circuit for P-MOSFET Buck converter High side Switching

Merit : Stable for large values of Input Voltages fluctuations, can be used for higher switching frequencies and External Gate driver IC is not required which could result in cost.

deMerit : number of Components required is very high however by choosing SMD components size and cost of the circuit can be minimised .

After evaluating the merits and demerits of the six circuits, Circuit-1 and Circuit-6 appear to be the most suitable options for the project in terms of their working principle, cost, and space requirements. Among two, Circuit-6 seems to be the easiest to implement, and therefore, it has been chosen as the final circuit for the project.

With the Circuit-6 as final gate Driver the Buck based MPPT charge converter is designed and Tested as shown in fig-4.19

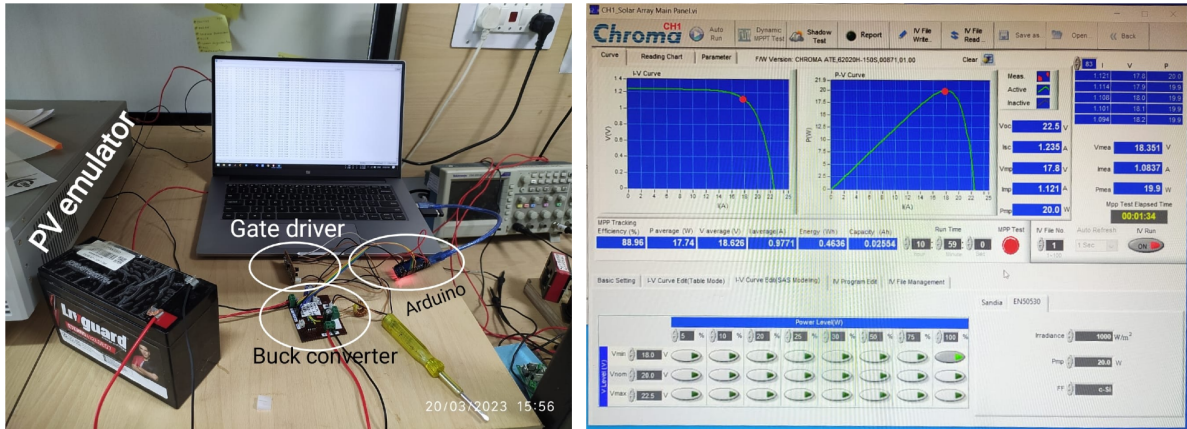


Figure 4.19: Setup for Buck converter based MPPT charge controller and results

the Buck converter is realised with circuit-6 so use of FAN739 as gate driver is point less so TC4427COA gate driver was chosen due to its outstanding performance characteristics and features. The TC4427COA offers high-speed switching capability, wide operating voltage range (4.5V to 18V), and low output impedance, ensuring efficient and reliable operation of the low side switch. Its simple pinout and surface-mount package make it easy to integrate into the circuit design, saving time and effort during the project implementation.

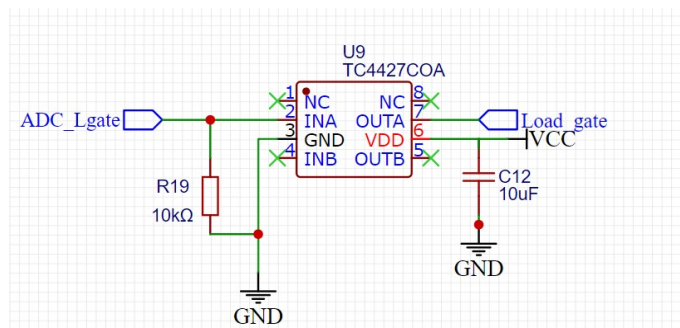


Figure 4.20: Gate driver circuit for Boost-converter N-MOSFET Low side Switching

4.6 Project Schematic

By Considering all the above parameters and adding other passive components such as decoupling, filter capacitors, pulldown resistors etc.. Complete schematic of the Project as show below

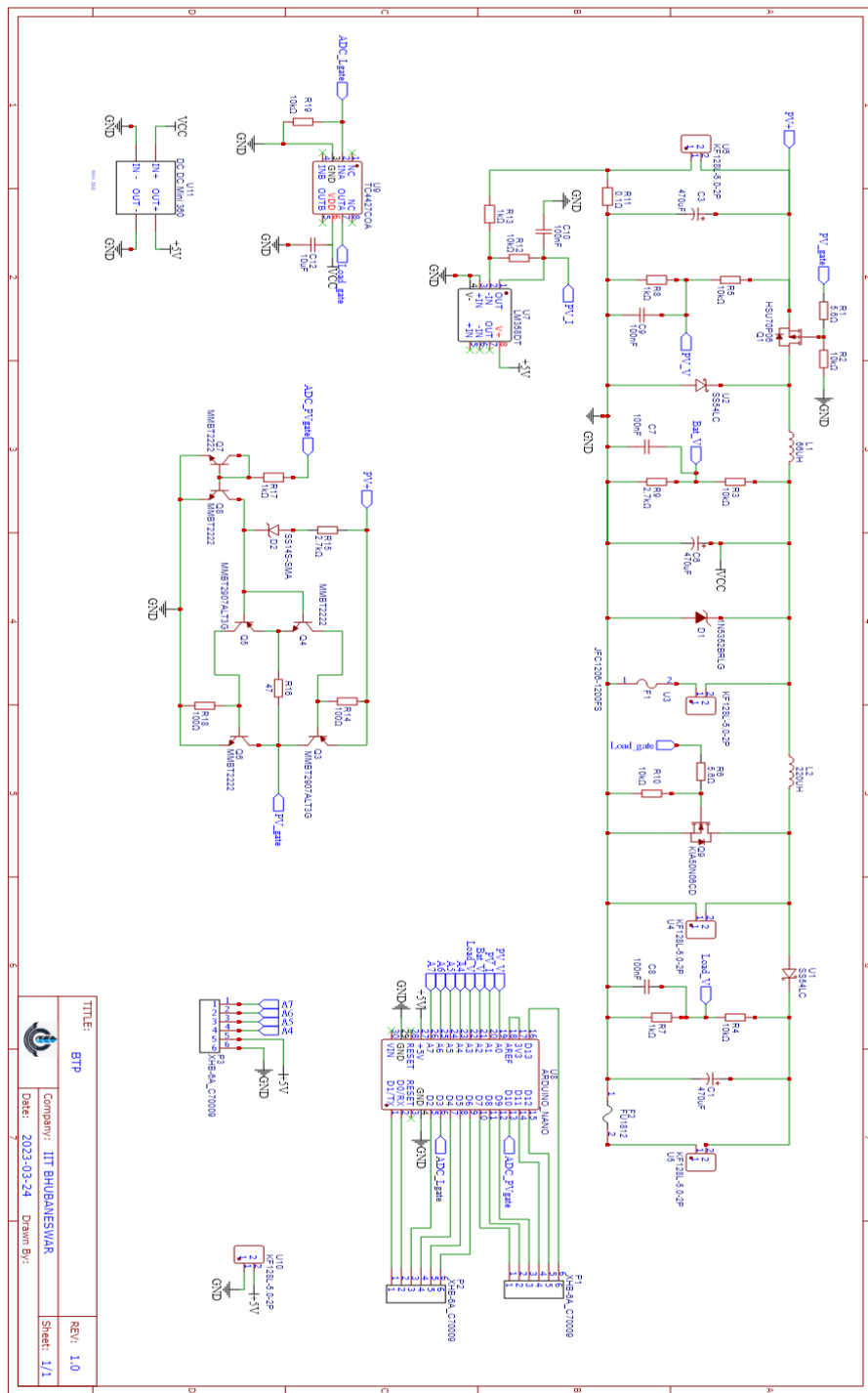


Figure 4.21: Project Schematic

4.7 PCB Designing

After completing the schematic, the next step in converting the circuit to a PCB involves defining the board outline. Once the board outline is established, the components are arranged inside the outline on both the top and bottom layers, taking into consideration space allocation and placement of sensitive components near IC chips for noise filtering. The PCB traces are then manually routed using the top and bottom layers to connect pads according to the net wires. The board outline can be adjusted as needed, and vias can be used when transitioning between layers. Additionally, copper pours can be incorporated for various advantages such as grounding, heat sinking, EMI shielding, copper balance, and providing short return paths for high current devices, depending on the specific requirements of the PCB design.

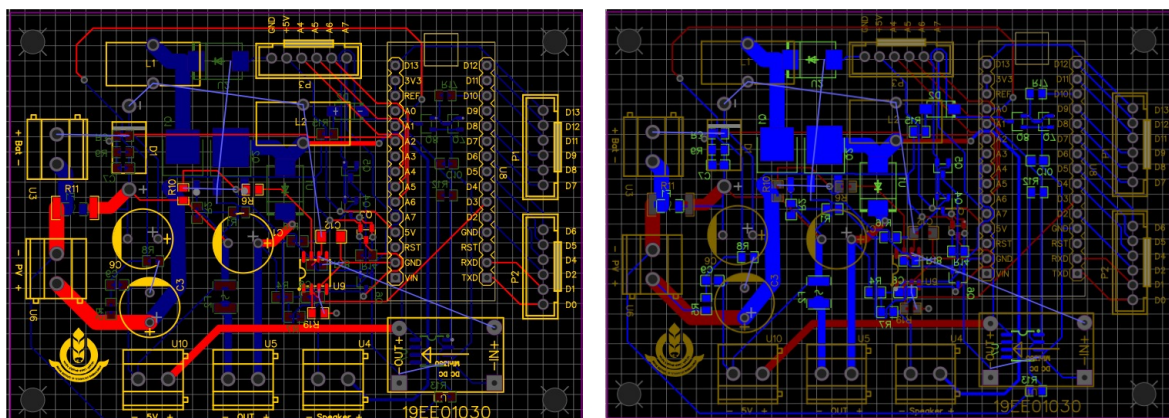


Figure 4.22: Snapshot of PCB layout while designing for the Project

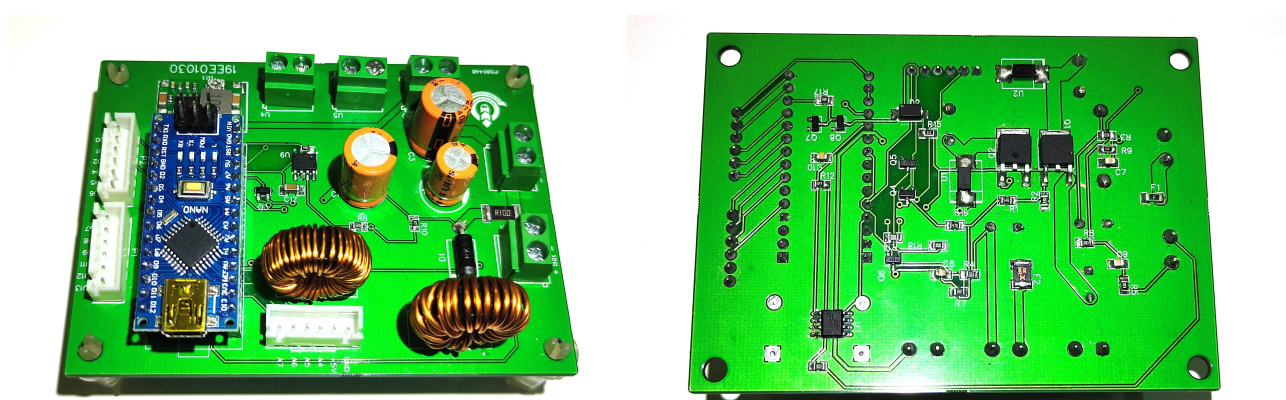


Figure 4.23: Project PCB after fabrication and Components assembly

4.7.1 Specifications

List of Materials(LOM)		
Name	Designator	Footprint
470uF Electrolytic Capacitor	C1,C3	CAP-TH_BD10.0-P5.00-D0.6-FD
470uF Electrolytic Capacitor	C6	CAP-TH_BD10.0-P5.00-D1.0-FD
100nF Ceramic Capacitor	C7,C9,C10,C8	C0805
10uF Ceramic Capacitor	C12	C1206
1N5352BRLG 5W Zener diode	D1	DO-27_BD5.2-L8.9-P12.90-D1.5-RD
SS14S-SMA Schottky Diode	D2	SMA_L4.3-W2.6-LS5.0-RD
JFC1206 5A Fuse	F1	F1206
FU1812 2A PPTC Fuse	F2	F1812
66UH 5A inductor	L1	IND-TH_L15.5-W7.2-P6.40-D1.0
220UH 3.3A inductor	L2	IND-TH_L15.5-W7.2-P6.40-D1.0
XHB-6A JST Connector	P1,P2,P3	CONN-TH_6P_XHB-6A
HSU70P06 P-MOSFET	Q1	TO-252-2_L6.6-W6.1-P4.58-LS9.9-BR
MMBT2907 PNP BJT	Q3,Q5	SOT-23-3_L2.9-W1.3-P1.90-LS2.4-BR
MMBT2222 NPN BJT	Q4,Q6,Q7,Q8	SOT-23-3_L2.9-W1.4-P1.91-LS2.6-BR
KIA50N06CD N-MOSFET	Q9	TO-252-2_L6.6-W5.7-P4.6-LS9.9-BR-CW
5.6Ω	R1,R6	R0805
10kΩ	R2,R3,R4,R5,R10,R12,R19	R0805
1kΩ	R7,R8,R13,R17	R0805
2.7kΩ	R9	R0805
0.1Ω	R11	R2512
100Ω	R14,R18	R0805
2.7kΩ	R15	R0805
47Ω	R16	R0805
SS54 5A Schottky Diode	U1,U2	DO-214AB_L6.9-W5.9-LS7.9-RD
KF128L-5.0-2P Screw Terminal	U3,U4,U5,U6,U10	CONN-TH_P5.00_KF128L-5.0-2P
LM358DT OP-amp	U7	SOIC-8_L5.0-W4.0-P1.27-LS6.0-BL
ARDUINO_NANO	U8	COMM-TH_ARDUINO_NANO
TC4427COA Gate Driver	U9	SOIC-8_L5.0-W4.0-P1.27-LS6.1-BL
Mini 360 Buck converter	U11	DC_DC_MINI360

Figure 4.24: List of Materials used in the Project PCB

Absolute Max PV Input Voltage	40	V
Operating PV Input Voltage	14-33	V
Absolute Max Battery Voltage	15.2	V
Operating Battery Voltage	10-14	V
Absolute Max Load Voltage	40	V
Operating Load Voltage	14-33	V
Max Operating PV Input Current	3.3	V
Absolute Max Battery Current (Bi directional)	5	A
Absolute Max Load Current	2.5	A

Table 4.2: Specifications of the Project Prototype

4.8 Other Features of the board

The Prototyped board has been meticulously designed with future scope in mind, incorporating various features to enhance its functionality. One such feature is a 5V 2A buck converter on board, which can be utilized to power image detection sensors, image processors, and even charge mobile devices such as smartphones. This makes the board versatile and capable of catering to a wide range of applications.

Furthermore, the board also includes ample GPIO pins that can be utilized for various purposes, such as PWM (Pulse Width Modulation) and measurement. With 12 output pins and 4 ADC (Analog-to-Digital Converter) pins available, external sensors and indicators, such as battery percentages and charging status, can easily be integrated into the system. This allows for convenient monitoring and control of different aspects of the system.

In addition, the board also supports I2C (Inter-Integrated Circuit) and SPI (Serial Peripheral Interface) communication, providing flexibility for integration with external displays and image microprocessors. This allows for seamless data transfer and communication between different components of the system, enabling efficient data processing and image analysis.

Overall, the Prototyped board is designed with a forward-thinking approach, incorporating various features such as the 5V 2A buck converter, ample GPIO pins, and I2C/SPI communication, to provide a versatile and powerful platform for a wide range of applications in the field of image detection, image processing, and mobile device charging.

Chapter 5

Testing

5.1 MPPT Testing

The Buck MPPT Test is done on prototype by using Chroma 62000H-S (Solar Array Simulator DC Power Supply) to simulate a PV panel to charge a 12V Nominal Lead acid battery

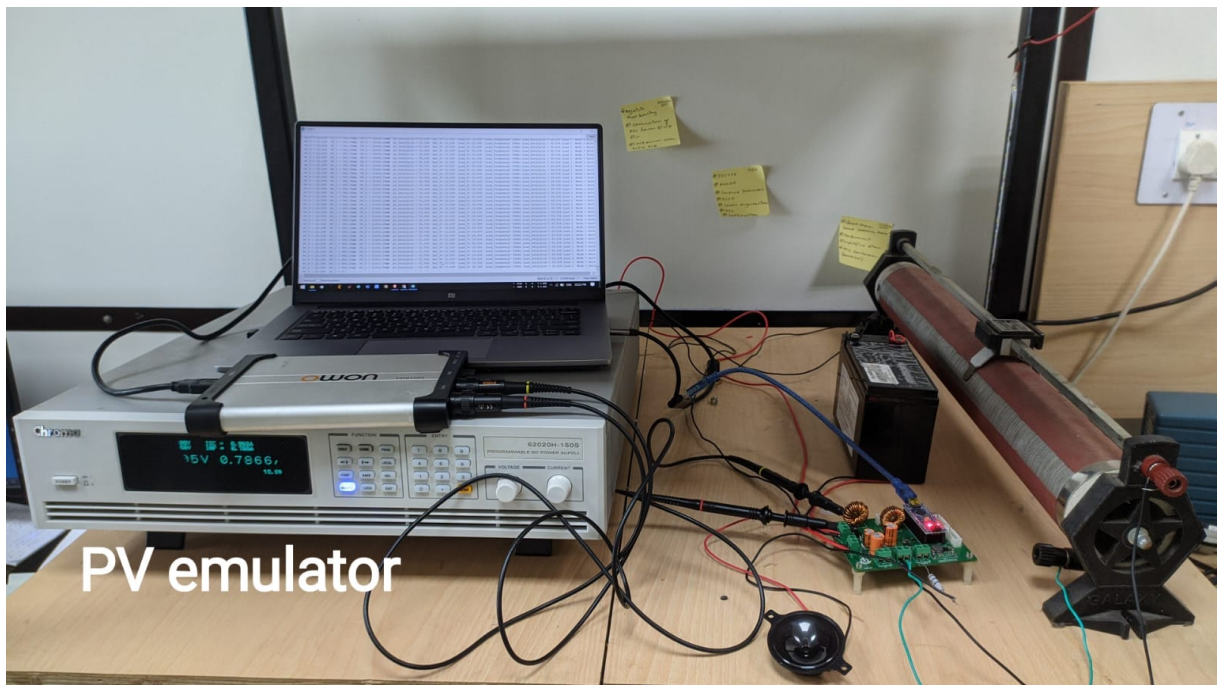


Figure 5.1: Experimental Setup for MPPT and Load Test

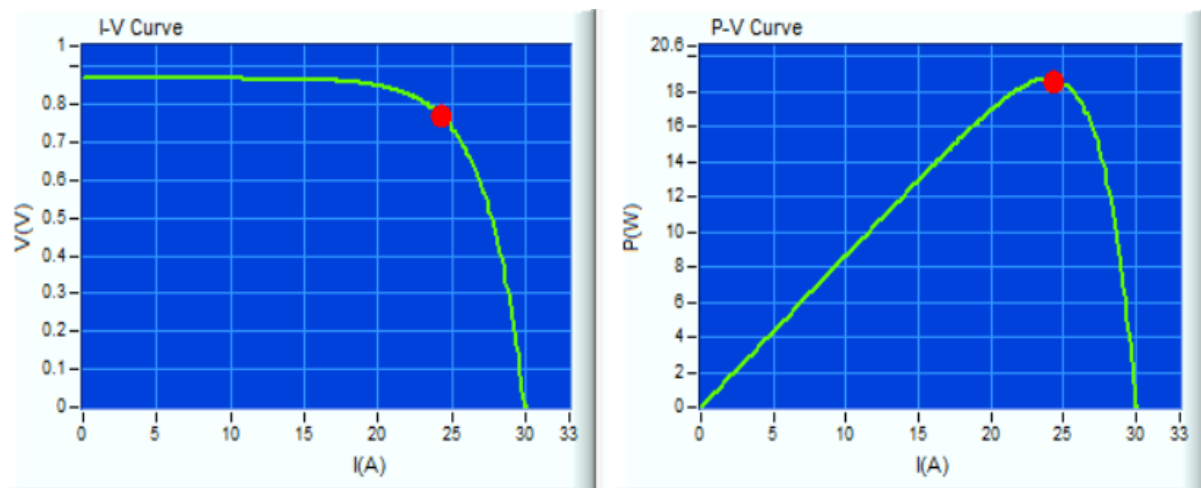
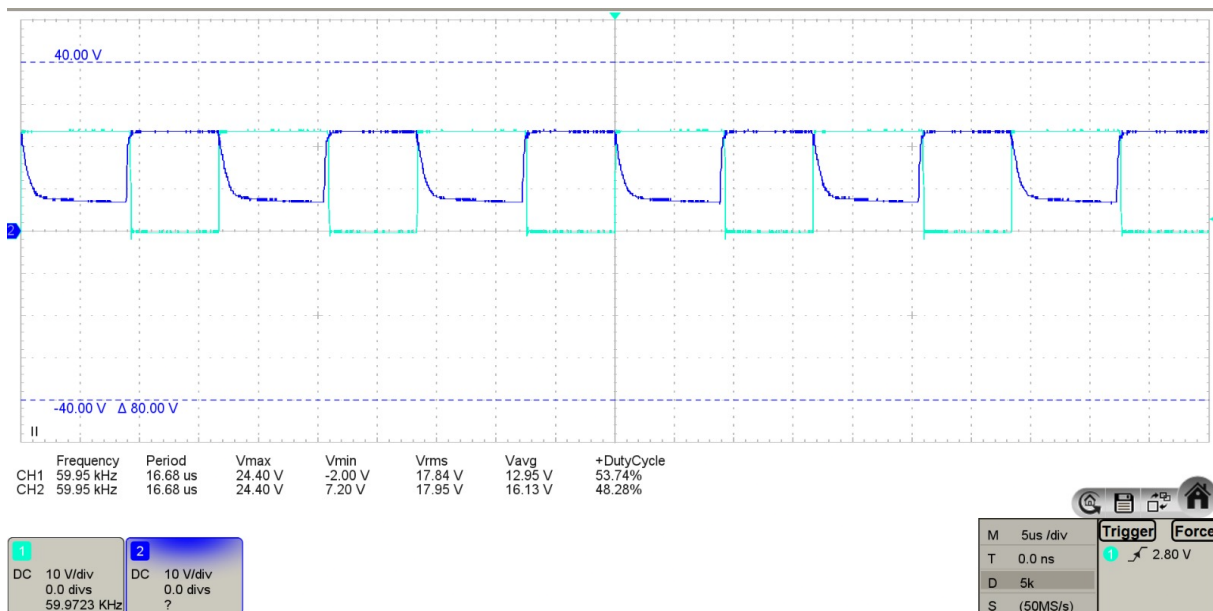
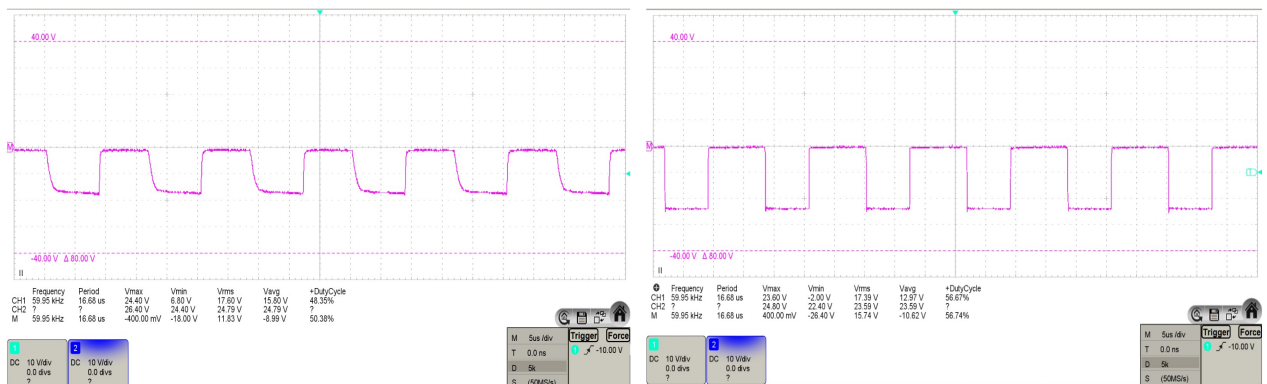


Figure 5.2: Results For MPPT Test

Figure 5.3: V_D (Azure) & V_G (Blue) with respective ground for PV Buck converterFigure 5.4: V_{GS} (Left) & V_{DS} (Right) for PV Buck converter

5.2 Boost converter & ultrasonic speaker Testing

Boost converter is tested with a Input battery voltage of 12V and a constant output voltage of 20V with ultrasonic speaker connected across the V_{DS} of the MOSFET and Tested the V_{Out} characteristics on constant switching frequency and Sweeping frequency.

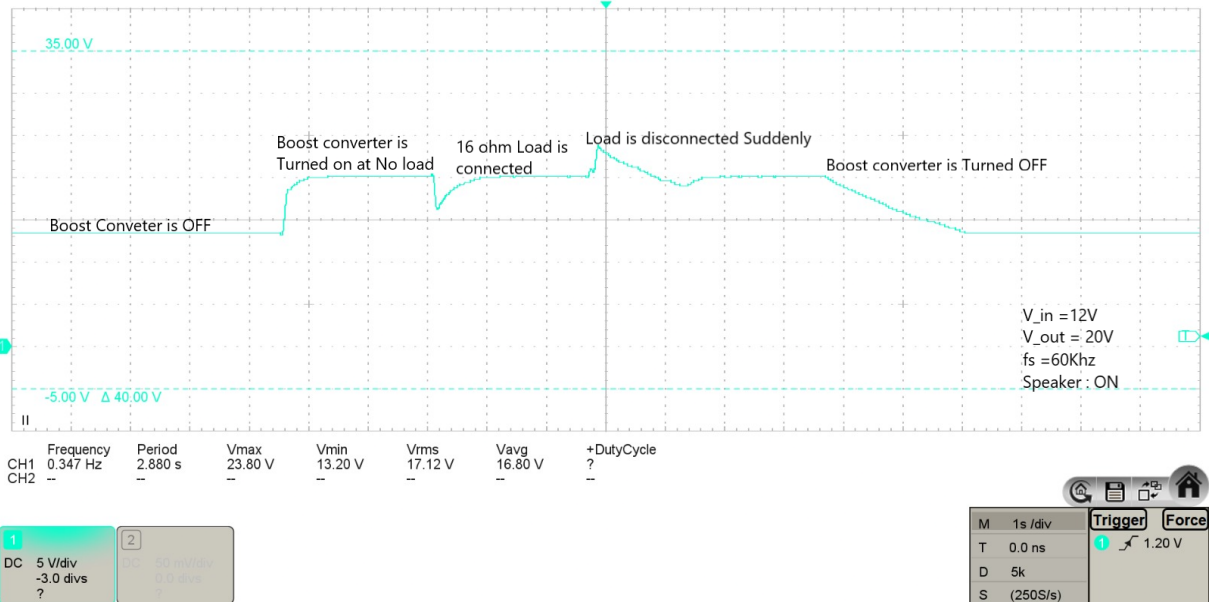


Figure 5.5: V_{out} characteristics @ 60Khz

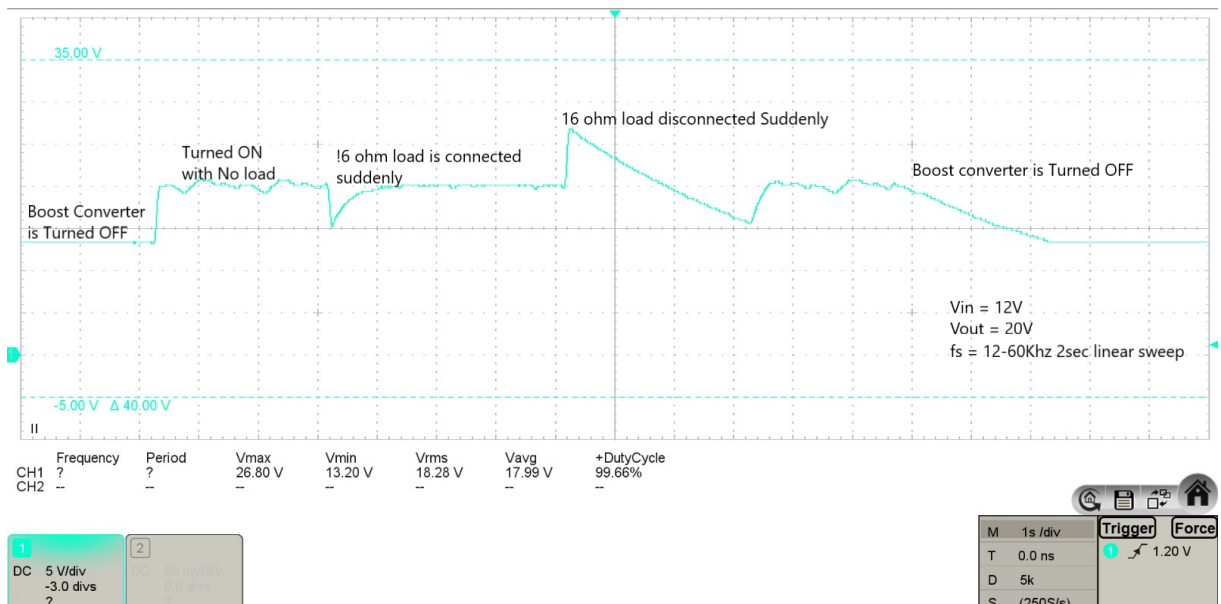


Figure 5.6: V_{out} characteristics @ $f_s = 12-60Khz$ of 2 sec repeated Linear sweep

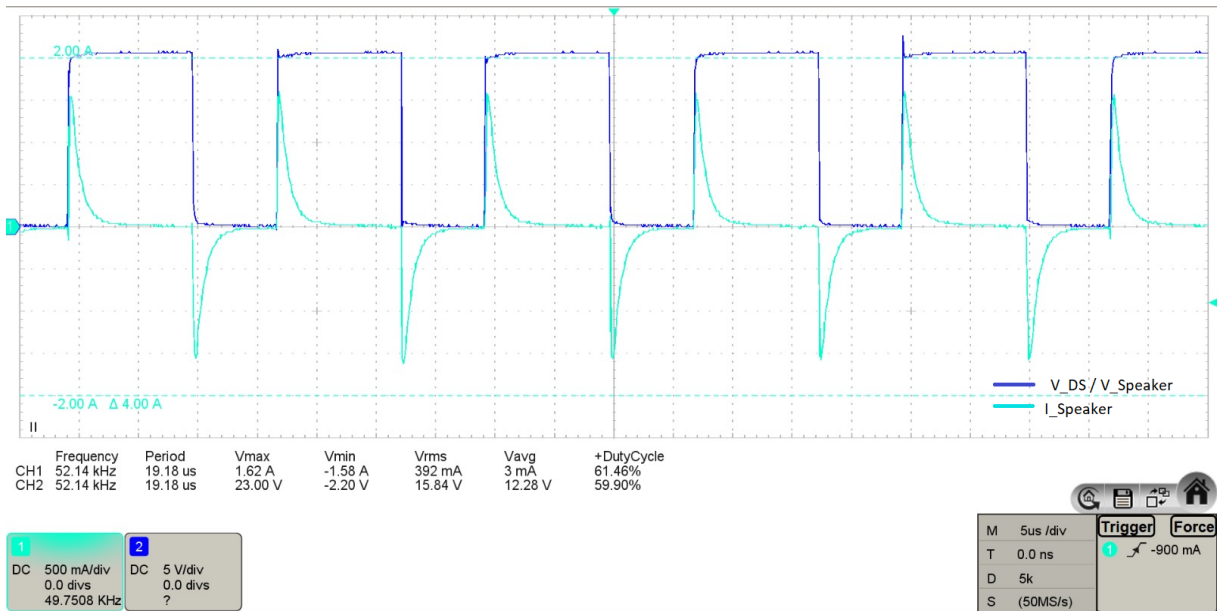
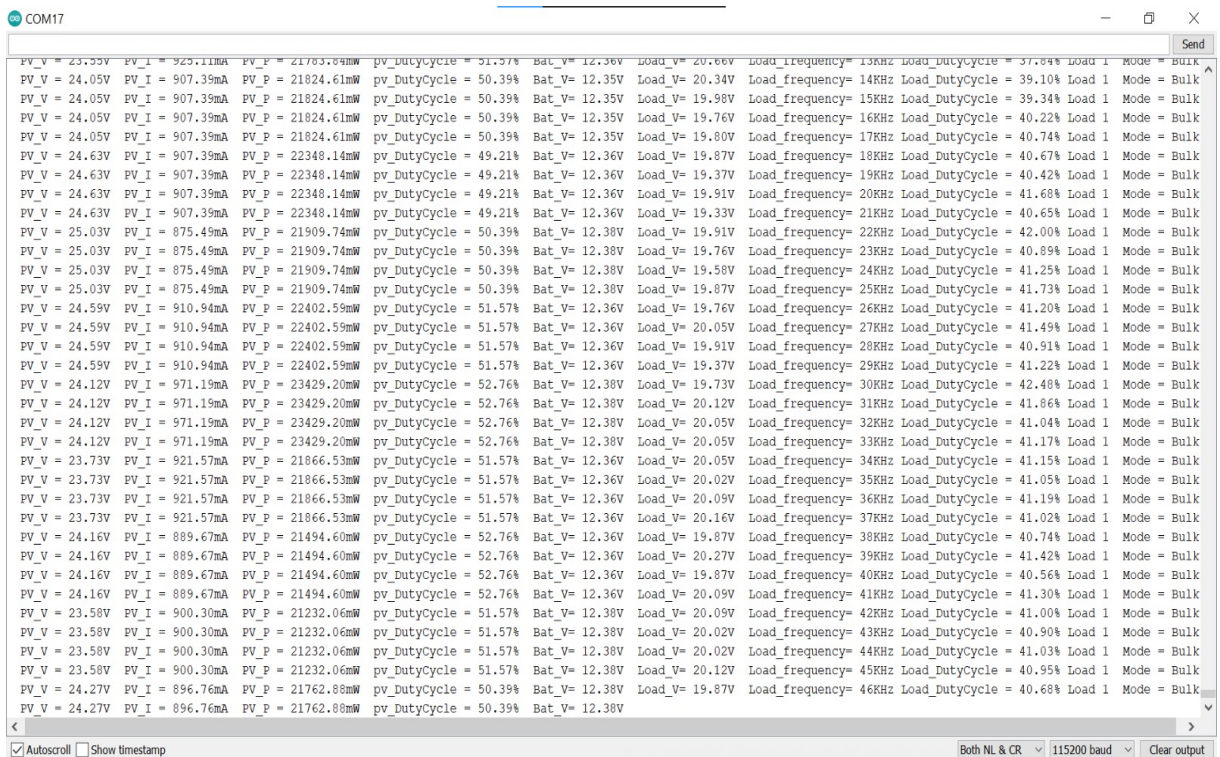
Figure 5.7: $V_{DS} / V_{Speaker}$ & $I_{Speaker}$ vs Time

Figure 5.8: Parameter Readings from Arduino Serial Monitor

5.3 Testing On Animals

The prototype was tested on domestic animals, such as dogs and cats, with modifications to ensure animal welfare. Measures were taken to ensure that **no animals were harmed during the experiment**, and the sound intensity used in the prototype was kept at a safe level of 70dB for the animals being tested. This was achieved by carefully considering the well-being of the animals and following applicable laws, regulations, and ethical guidelines for animal testing. The variable frequency ultrasonic sound generator was controlled wirelessly through a smartphone, and the DAC value of the ESP32 connected to the ADC of the Arduino Nano was adjusted accordingly. The input ADC values were mapped to frequencies ranging from 10 kHz to 60 kHz. Thorough testing of the modified prototype was conducted to ensure proper functionality and safety before proceeding with animal testing. Clear documentation of the experimental setup, data collection, and analysis procedures was maintained, and the results were reported transparently, including any limitations or uncertainties associated with the study. It is important to prioritize the welfare of animals in all research and testing activities and to adhere to ethical considerations, safety precautions, and relevant guidelines.

For more detailed video of the experiment visit : https://www.youtube.com/watch?v=_Kgu1dhLU2Y

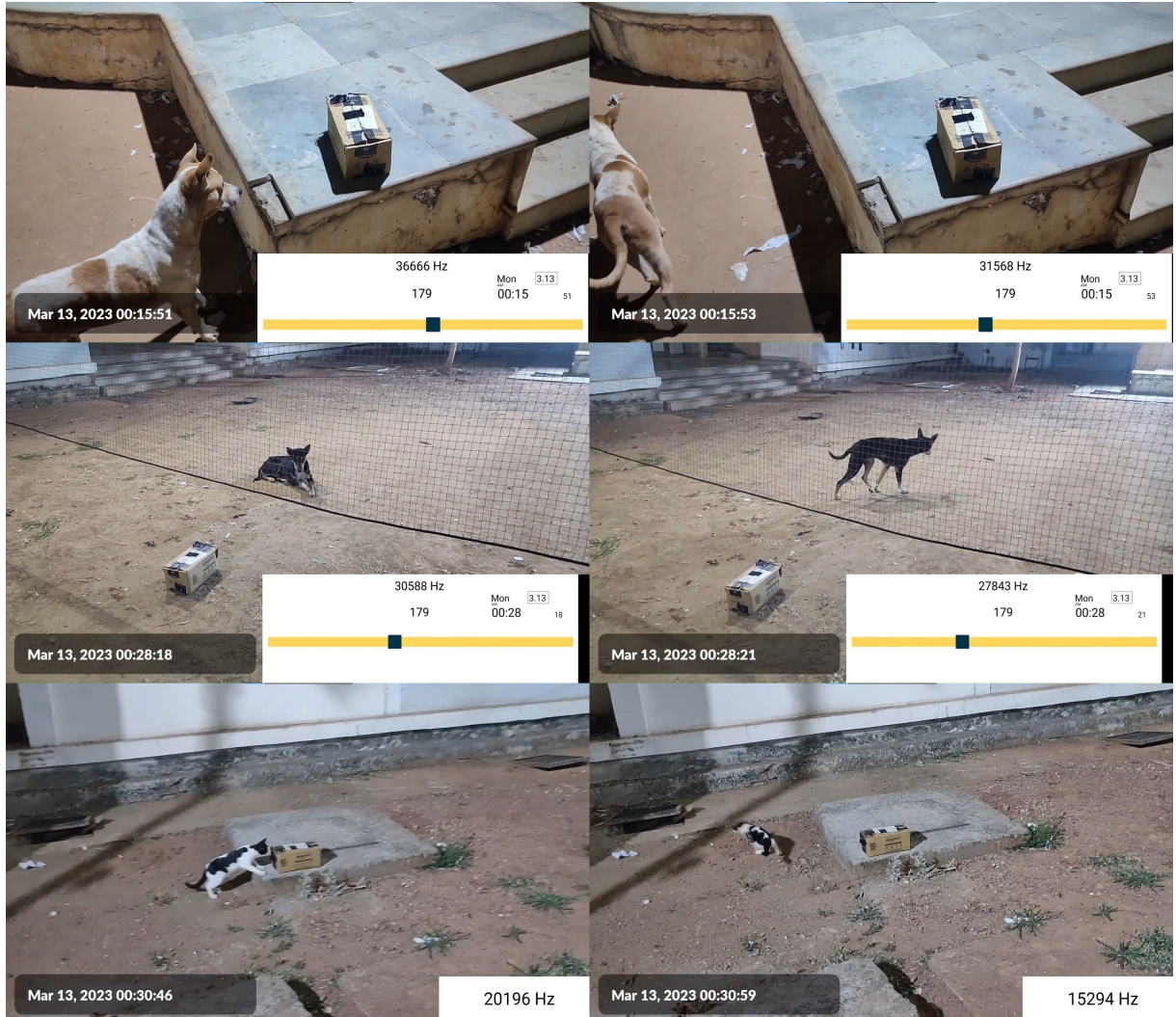


Figure 5.9: Ultrasonic Test On animals representing animal deterrence to Ultrasonic Sound

Chapter 6

Code Overview & Functionality

The code is written in Arduino language and is intended to be used in a solar power management system. The system comprises a solar panel (PV), a battery, and a load. The purpose of the code is to regulate the charging and discharging of the battery, as well as control the load voltage, based on various parameters.

The code begins by defining several constants that determine the behavior of the system. These constants include the load reference voltage, which specifies the desired voltage for the load. This value serves as a reference for the system to maintain the load voltage at the desired level.

The code also includes constants for the start and end frequencies of an ultrasonic sound sweep. This sound is generated by a speaker connected across the Vds (drain-source voltage) of the load converter. The sweep frequency range and the delay between frequency sweeps are also defined as constants, along with the increment value for changing the frequency. These parameters control the frequency at which the ultrasonic sound is swept, which is used as a feedback mechanism in the system.

Furthermore, the code includes PID (Proportional-Integral-Derivative) controller coefficients for load voltage control. PID is a feedback control algorithm that adjusts the output based on the error between the reference voltage and the actual voltage. The

coefficients determine the response of the PID controller and help regulate the load voltage by adjusting the duty cycle of the PWM signal.

Additionally, the code includes constants for the solar panel (PV) switching frequency and sample time for Maximum Power Point Tracking (MPPT). MPPT is a technique used to optimize the power output of the PV panel by tracking its maximum power point, which is the point where the panel generates the most power. The battery voltage thresholds for different charging modes, such as bulk charging, absorption charging, and float charging, are also defined as constants. Moreover, maximum and minimum current limits for different charging modes are set as constants to ensure safe charging of the battery.

The code utilizes variables to store PV parameters, such as voltage and power change rate, as well as the battery voltage. These variables are updated during the main loop of the code, which runs continuously. The PV parameters are used to calculate the MPPT and determine the appropriate charging mode for the battery based on its voltage level.

The code also initializes timers for Pulse Width Modulation (PWM) and sets the PWM output pins as outputs. PWM is used to control the charging and discharging of the battery by regulating the duty cycle of the PWM signal. The duty cycle determines the amount of time the battery is charged or discharged, and it is adjusted based on the PID controller output to regulate the load voltage.

In summary, the provided code implements a control algorithm that manages the charging and discharging of a battery in a solar power management system. It uses feedback from the load voltage and solar panel parameters, along with a PID controller, to regulate the load voltage, optimize the power output from the solar panel, and ensure safe charging of the battery.

code: [https://github.com/Jishnusyam/B-Tech-Project-19EE01030-](https://github.com/Jishnusyam/B-Tech-Project-19EE01030)

Conclusion

In this B-tech Project, we have proposed an innovative solution for animal deterrence using a PV-powered ultrasonic sound generator. The system offers a humane and eco-friendly approach to addressing human-wildlife conflict, including road/railway accidents and crop damage. The ultrasonic sound generated by the system does not cause harm to animals and is not audible to humans, making it an ideal solution for wildlife conservation efforts.

The proposed system has several advantages over traditional animal deterrence methods. It does not rely on external power sources, as it is powered by a solar panel and battery, making it suitable for remote areas and wildlife habitats with limited access to electricity. It has the potential to reduce animal casualties from road/railway accidents by deterring animals from high-risk areas, protecting both animals and humans. Additionally, it can help farmers mitigate crop losses by protecting crops from animal damage.

The system architecture includes a solar panel, MPPT charge controller, battery, and ultrasonic speaker amplifier. Field trials can be conducted to evaluate the effectiveness of the system in deterring animals and preventing wildlife-related incidents. The results of these trials can be analyzed to determine the efficacy of the system and its potential for widespread implementation in wildlife conservation efforts and human-wildlife conflict mitigation.

Overall, the PV-powered ultrasonic sound generator presents a promising solution for animal deterrence, with implications for wildlife conservation, crop protection, and

wildlife management. This innovative approach has the potential to contribute to the field of animal deterrence research and practice, and it can aid in mitigating human-wildlife conflicts globally. Further research and testing can be conducted to refine the system and explore its applications in different settings to address the growing challenge of human-wildlife conflict worldwide.

Bibliography

1. APHIS [Animal Plant Health Inspection Service] Regulation of agricultural animals (policy 26). In: Animal Care Resource Guide. Washington, DC: US Department of Agriculture; 1998.
2. Motzel SL, Morrisey RE, Conboy TA, et al. Weight loss in rats associated with exposure to infrasound. *Contemp Topics*. 1996;35:69.
3. NRC [National Research Council] Guide for the Care and Use of Laboratory Animals. 7th ed. Washington, DC: National Academy Press; 1996. [PubMed]
4. Sales GD, Milligan SR. Ultrasound and laboratory animals. *Anim Technol*. 1992;43:89-98.
5. . D.Shah, Sharma, “Practical Detection Of Animal And Collision Avoidance System Using Computer Vision Technique” IEEE 2017
6. Luis obrega, andre tavares, Antonio Cardoso, pedro goncalves, IEEE 2018, “Animal Monitoring Based On Iot Technologies”
7. Kanad Roy, Subhendu Mazumdar ”Recent Trends in Environmental Science and Applied Ecology (pp.89-98) Publisher: Bhumi Publishing”